

Changes in the Flux of Nitrate during Storms in an Eastern Shore, Virginia Stream

Jennifer E. Ren  
Charlottesville, Virginia

A Thesis presented to the Faculty  
of the University of Virginia  
in Fulfillment of the  
Distinguished Majors Program

Department of Environmental Sciences

University of Virginia  
May 2015

---

Aaron L. Mills,  
Thesis Advisor

---

Janet S. Herman,  
Thesis Co-Advisor

---

Thomas M. Smith  
Director of Distinguished Major Program

## Abstract

During a storm event, transient changes in the hydraulic gradient can result in very different discharge rates, residence times of bank storage, and ultimately  $\text{NO}_3^-$  concentrations in the stream. During varying storm events, water samples were collected with an automatic storm sampler and hydraulic gradient fluctuations between the stream and stream bank were measured with pressure transducers. In the nine storms sampled,  $\text{NO}_3^-$  concentrations generally decreased during the passing of a flood wave. Furthermore, flood wave height and duration together controlled  $\text{NO}_3^-$  flux during the storm as there was a strong positive relationship between the change in  $\text{NO}_3^-$  flux when compared with base flow and the total storm discharge when compared with base flow. Small flood waves with small discharges resulted in a decrease in  $\text{NO}_3^-$  flux during the storm. Slower discharges created longer residence times for more  $\text{NO}_3^-$  removal. Large flood waves ultimately resulted in an increase in  $\text{NO}_3^-$  flux, although large flood waves with different flood durations had vastly different increases in  $\text{NO}_3^-$  flux. Short durations created high rainfall intensities which reduced head gradients, discharge and  $\text{NO}_3^-$  flux. Conversely, long durations created low rainfall intensities which increased head gradients, discharge and  $\text{NO}_3^-$  flux. These results provide better insight into  $\text{NO}_3^-$  transport into streams and will inform better models to help predict future watershed  $\text{NO}_3^-$  budgets.

## Table of Contents

Abstract.....	i
List of Figures and Tables.....	iv
Acknowledgements.....	vi
Chapter 1. Introduction .....	1
1.1 Purpose.....	1
1.2 Problem Statement .....	1
1.3 Technical Approach .....	3
1.4 Review of Technical Literature.....	4
1.4.1 Lowering of Nitrate Concentration.....	4
1.4.2 Storm Mechanics .....	5
1.5 Objectives.....	8
Chapter 2. Methods.....	9
2.1 Sampling Location .....	9
2.2 Collection of Water Samples.....	10
2.3 Analysis of Water Samples .....	11
2.4 Determination of Combined Hydrograph and Hyetograph.....	12
2.4.1 Stream stage.....	12
2.4.2 Precipitation.....	13
2.5 Determining Change in Discharge and Nitrate Flux.....	14
2.6 Hydraulic Gradients .....	15
2.7 Storm Intensity and Duration .....	16
Chapter 3. Results .....	17
3.1 Summary of Storm Events Captured.....	17
3.2 Stream Stage, Nitrate Concentration, and Precipitation.....	18
3.3 Head Gradients.....	26
3.4 Effects of Storm Intensity and Duration on Nitrate Flux .....	29
Chapter 4. Discussion .....	34

4.1 Influence of Hydraulic Gradients on Discharge and Nitrate Concentration .....	34
4.2 Effects of Storm Intensity and Duration on Nitrate Flux .....	36
4. 3 Patterns in non-storm events .....	40
4.4 Project Relationship to Larger Scope.....	41
4.5 Future Research.....	42
References .....	44

## List of Figures and Tables

Figure 1.1	Schematic illustration of the difference between large and small flood waves...	7
Figure 2.1.	Location of Cobb Mill Creek in Virginia and the hillslope within the Cobb Mill Creek Watershed.....	9
Figure 2.2	Schematic of the stage-activated automatic sampler for collecting stream water at regular intervals during storms. From [ <i>Gu et al.</i> , 2008].....	10
Figure 2.3	Rating curve for the culvert gauge at Cobb Mill Creek. From [ <i>Pickus et al.</i> , 2014].....	15
Table 3.1	Summary of storm events illustrating properties of all the storms captured.....	18
Figure 3.1	Storm starting on October 22, 2014.....	19
Figure 3.2	Storm starting on November 1, 2014.....	20
Figure 3.3	Storm starting on November 17, 2014.....	21
Figure 3.4	Storm starting on December 24, 2014.....	22
Figure 3.5	Storm starting on December 29, 2014.....	23
Figure 3.6	Storm starting on January 12, 2015.....	23
Figure 3.7	Storm starting on January 18, 2015.....	24
Figure 3.8	Storm starting on February 2, 2015.....	24
Figure 3.9	Storm starting on February 9, 2015.....	25
Figure 3.10	Non-storm event on July 11, 2014.....	25
Figure 3.11	Non-storm event on September 27, 2014.....	26
Figure 3.12	Stream stage, water table elevation and hydraulic gradient during storm starting October 22, 2014.....	27
Figure 3.13	Stream stage, water table elevation and hydraulic gradient during storm starting November 1, 2014.....	28
Figure 3.14	Stream stage, water table elevation and hydraulic gradient during storm starting November 17, 2014.....	29

Figure 3.15	Storm duration (h) of storms captured between October 22, 2014 and January 20, 2015 plotted against their respective changes in nitrate flux (kg).....	30
Figure 3.16	Flood wave duration (h) of storms captured between October 22, 2014 and January 20, 2015 plotted against their respective changes in nitrate flux (kg)....	30
Figure 3.17	Total precipitation (mm) of storms captured between October 22, 2014 and January 20, 2015 plotted against their respective changes in nitrate flux (kg)....	31
Figure 3.18	Peak hourly intensity ( $\text{mm hr}^{-1}$ ) of storms captured between October 22, 2014 and January 20, 2015 plotted against their respective changes in nitrogen flux (kg).....	32
Figure 3.19	Change in discharge of storms captured between October 22, 2014 and January 20, 2015 plotted against their respective changes in nitrogen flux (kg).....	32
Figure 3.20	Flood wave height of storms captured between October 22, 2014 and January 20, 2015 plotted against their respective changes in nitrogen flux (kg).....	33
Figure 4.1	Hydraulic gradient, nitrate concentration in hourly samples, and continuous discharge for the storm event on November 17, 2014.....	35
Figure 4.2	Linear relationship between total precipitation (mm) and height of flood wave (cm).....	36

## Acknowledgements

I would like to thank and express my deepest appreciation to Dr. Aaron Mills and Dr. Janet Herman for their invaluable guidance on my research project. Foremost, I would like thank Aaron for his enthusiasm and dedication over the past year. Despite his busy schedule, he has always made himself available and helped me in all phases of this research project, from data collection to scientific writing. I would also like to thank Dr. Janet Herman for her encouraging spirit and invaluable knowledge. I greatly appreciate Ami Riscassi for showing me how to use an ISCO sampler and for letting me borrow her stage activator. I would also like to thank the DMP committee for their guidance through this DMP process and thanks to the Anheuser-Busch Coastal Research Center and Virginia Coast Reserve Long Term Ecological Research Program (NSF DEB-0621014) for providing field accommodations and logistical support for this project.

I would also like to thank my friends and research team members, Ben Pickus and Cassie Cosans for their support. I will always remember our fun trips to the Eastern Shore, drenching ourselves in bug spray, and eating like kings after a hard day's work. I would also like to thank Oliver Goodridge for making multiple trips to the Eastern Shore with me and helping me retrieve my water samples.

Lastly, I would like to give a special thank you to Mr. David Boyd for taking time in his busy schedule and helping me reload ISCO bottle trays, checking battery life, bagging and refrigerating my water samples for me while I was in Charlottesville. I would never have acquired so many storm samples without his help. His tireless dedication and generosity are sincerely appreciated.

## Chapter 1. Introduction

### 1.1 Purpose

Most studies on nitrate removal have focused on steady state conditions [Chen, 2007; Gu 2007, Flewelling et al., 2012; Robertson, 2009] while this thesis seeks to understand what occurs during transient conditions such as storm events. The goal was to understand how storm intensity and duration affect nitrate flux as compared to base flow conditions. Using field data collected during nine storm events, nitrate flux was compared with storm-associated properties including flood wave height, discharge, and flood duration. The information gained from this project provides better insight into  $\text{NO}_3^-$  transport into streams and has the potential to better model future nitrate watershed budgets.

### 1.2 Problem Statement

Nitrogen is one of the most common agricultural contaminants in groundwater and surface water around the world [Galloway and Cowling, 2002]. It affects 40% of the rivers and 57% of the estuarine systems in the United States [USEPA and USDA, 1998]. Fertilizer practices have been associated with this widespread contamination of nitrogen. The use of inorganic nitrate fertilizers has become a common choice for farming communities, because fertilizers such as ammonium nitrate are inexpensive and significantly increase crop yield [Smil, 1997; Evans, 1996 as cited in Robertson, 2009]. From 2003 to 2006, the United States used 12.5 million tons of nitrogen-based fertilizer generating an excessive amount of nitrate in our water resources [Wiebe and Gollehon, 2006].

Due to its high solubility, nitrogen (especially  $\text{NO}_3^-$ ) from agricultural activities can easily leach from croplands in coastal plain settings into the groundwater and eventually into

streams, coastal lagoons, and bays [*Denver, 1989; Speiran, 1996; Bachman et al., 1998; Flewelling et al., 2011*]. This nitrate contamination can have harmful effects on the health of humans as well as the function of ecological systems. For one, high levels of nitrate in drinking water can cause methemoglobinemia, a disorder that prevents oxygenation of the blood and tissue and can be fatal [*Roberston, 2009*]. The effects on human health of low levels of nitrate in drinking water are uncertain, but initial studies have correlated long-term low-level nitrate exposure to reproductive health issues and colon cancer [*Croen et al., 2001 as cited in Roberston, 2009*]. Regarding ecological systems, nitrate contamination can cause eutrophication of surface waters. Nitrate promotes growth of aquatic plants such as algae as well as crops in agricultural systems, and in the former the result is degradation of the system through eutrophication. Excessive nitrate in water systems creates algal blooms that block out sunlight for other plants to conduct photosynthesis. As the algal blooms die and decompose, they create zones that are hypoxic or anoxic, depleting dissolved oxygen in the water [*Hill, 1997 as cited in Robertson, 2009*]. Hypoxia induced by eutrophication in the Chesapeake Bay has killed many fish [*Roberston, 2009*]

For shallow groundwater systems within the coastal-plain region of Virginia's Eastern Shore, groundwater is particularly vulnerable to nitrogen contamination [*Gu, 2007*]. Roughly half the nitrogen load in a stream is first stored in groundwater before being discharged through base flow in streams [*Phillips and Lindsey, 2003*] which then drain either to the Chesapeake Bay or to the seaside lagoons. Most drinking water on the Eastern Shore is drawn from the Eastover-Yorktown aquifer that underlies the unconfined Columbia. Nitrate (the dominant form of groundwater N) does not reach the lower aquifer in significant amounts such that nitrate-related health issues are not considered to be a major problem. However, roughly 25% of the population

draws its water from the unconfined aquifer which can contain  $\text{NO}_3^-$  concentrations well above the EPA standard for drinking water of  $10 \text{ mg L}^{-1} \text{ NO}_3^- \text{-N}$  [Mills, 2011] Interestingly, while the Chesapeake has serious eutrophication problems, eutrophication of bays and lagoons on the sea side of the peninsula has not occurred extensively thus far, but those waters are sensitive to contamination by nitrogen that enters them from terrestrial sources [McGlathery *et al.*, 2007]. The susceptibility of Virginia's Eastern Shore makes understanding the nitrogen processes through the groundwater/surface water interface (GSI), where potential for nitrogen removal has been demonstrated, of the utmost importance.

### 1.3 Technical Approach

The research reported here was conducted at Cobb Mill Creek, a second order, groundwater-fed stream on the Eastern Shore of Virginia. The biological activity in the stream sediments of Cobb Mill Creek has the potential to remove all  $\text{NO}_3^-$  from groundwater as it passes through them [Flewelling *et al.*, 2012; Williems *et al.*, 1997]. As noted in previous studies, nitrate removal is often efficient along shallow riparian groundwater flow paths [Lowrance, 1992; Vidon and Hill, 2004]. Exemplified from numerous sediment core studies in Cobb Mill Creek's stream bank profile, Flewelling *et al.* [2012], demonstrated a strong decline in  $\text{NO}_3^-$  concentration from  $15\text{-}20 \text{ mg NO}_3^- \text{-N L}^{-1}$  in the nearby groundwater to  $1\text{-}2 \text{ mg NO}_3^- \text{-N L}^{-1}$  in the stream. Nitrate-containing groundwater that discharges to Cobb Mill Creek through organic-rich streambed sediments can be reduced in  $\text{NO}_3^-$  concentration due to microbial denitrification (the conversion of  $\text{NO}_3^-$  to  $\text{N}_2$ ). The rate of nitrate removal by denitrification is largely controlled by the residence time of the advecting groundwater, which is, in turn, determined largely by near-stream hydraulic gradients [Gu *et al.*, 2008; Mills *et al.*, 2011; Flewelling *et al.*, 2012]. Longer residence times in the streambed sediments result in greater removal of nitrate [Gu *et al.*, 2008].

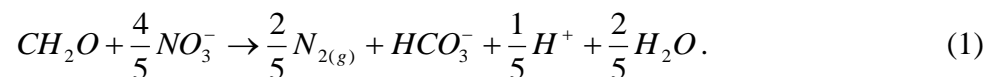
While the relationship between residence times and nitrate removal has been widely observed [Chen, 2007; Squillace, 1996; Gu 2007, Flewelling et al., 2012; Robertson, 2009], the impact of transient phenomena such as storm events on retention time, and hence,  $\text{NO}_3^-$  removal has not been well studied and is largely unknown [Cirimo et al. 1997]. The passage of a flood wave over sandy stream sediments can dramatically change the near-stream hydraulic gradient and, thereby, the nitrate flux across the groundwater surface water interface (GSI) [Gu et al., 2008].

## 1.4 Review of Technical Literature

### 1.4.1 Lowering of Nitrate Concentration

Microbial processes (including denitrification), plant uptake, and dilution are three major factors that can decrease nitrate concentration in a riparian environment. Through those processes, riparian buffers can remove up to 90% of the nitrate from shallow groundwater [Hedin et al. 1998].

The largest factor affecting nitrate reduction is denitrification, the conversion of  $\text{NO}_3^-$  to  $\text{N}_2$  [Zumft, 1997 as cited in Flewelling, 2009]. An estimated 63% of nitrate input in anaerobic lake bottom sediments can be removed via denitrification [Chen et al., 1972 as cited in Flewelling, 2009]. When oxygen is limited, anaerobic bacterium, use nitrate and nitrite as electron acceptors in the oxidation of organic matter. Nitrate is reduced through the following reaction [Freeze and Cherry, 1979]:



Because this reaction requires organic carbon and low oxygen, locations with high concentrations of dissolved organic carbon (DOC) and low dissolved oxygen are favorable for denitrification. These conditions are often found in riparian zones and streambeds of agricultural

watersheds, where nitrate-rich groundwater mix with DOC-rich groundwater or with organic-rich peat deposits [Flewelling, 2009; Hill et al., 2000; Hedin et al., 1998].

In addition to microbes, Hedin et al. [1998] found that riparian buffers, which include the trees and other vegetation that grow along the waterway, also promote denitrification in stream areas. The importance of vegetation in this buffer can be seen in the changes in nitrate removal patterns during different seasons. During summer months, vegetation actively undergoes evapotranspiration, a process by which vegetation consumes and loses water through a combination of evaporation and transpiration. Due to the availability of sunlight from the day to night, diurnal variation in the evapotranspirative demand of water arises. In shallow water tables, this demand of water draws down the water table beneath the vegetation [Robertson, 2009; Reid-Black, 2014]. As a result of this drawdown, the gradient between the stream and water table is reduced. A smaller gradient reduces the rate of discharge of the groundwater to the stream, increasing residence time in the zone of denitrification and, thus, increasing nitrate removal. Conversely in the fall and winter seasons, there is no draw down by evapotranspirative demand for water because vegetation is dormant. As a result, the gradient between the stream and the water table increases, the rate of groundwater discharge increases, residence time decreases and less nitrate is removed [Gribovski et al., 2008 as cited in Robertson, 2009].

Another way to decrease nitrate concentration is dilution. Nitrate dilution typically results from either precipitation or the mixing of low and high nitrate concentration groundwater [Lowrance et al. 1984]. When precipitation, that is void of nitrate, mixes with groundwater containing high concentrations of nitrate, the overall nitrate concentration is reduced.

#### **1.4.2 Storm Mechanics**

Gu et al. [2008] examined the transport and transformation of  $\text{NO}_3^-$  during simulated transient-flow events. During normal base-flow conditions, the stream-water surface was lower

than the nearby water table, and the resulting hydraulic gradient drove nitrate-containing groundwater discharge into the stream. However, during a storm event, transient changes in the hydraulic gradient due to changes in stream stage occurring more rapidly than changes in the nearby water table can result in very different discharges, residence times of bank storage, and ultimately nitrate concentrations in the stream [Gu *et al.*, 2008].

In the riparian aquifer of a forested catchment, Wondzell and Swanson [1996a, 1996b] measured water table fluctuations and nitrogen dynamics during storm events. They found that storms temporarily increased dissolved nitrogen in groundwater and enhanced nitrogen fluxes from the aquifer to the stream. This conclusion is further supported by the flushing hypothesis. Creed and Band [1996] suggested that a rapid addition of water during a storm flushes solutes stored in the groundwater out into the stream. Due to this rapid discharge, residence times might be insufficient for denitrification to occur. On the other hand, soils with low permeability might slow down the discharging water despite high hydraulic heads. Low permeability could even reverse hydraulic head gradients between the stream and the water table elevation [Sawyer *et al.*, 2014] (a situation referred to as bank storage).

According to Gu *et al.*'s [2008] modeling study, different sized flood waves can either increase or decrease  $\text{NO}_3^-$  flux (Figure 1.1). Small flood waves slow discharge through the sediment yielding a longer residence time. Concomitantly, more  $\text{NO}_3^-$  is removed, resulting in a lower flux of  $\text{NO}_3^-$  when compared with base flow.

Larger flood waves, however, can lead to an increase in  $\text{NO}_3^-$  flux to the stream. During a large storm event, the elevated stage can actually cause recharge of the groundwater in the sediments and stream banks. That recharge water is oxygenated and contains less  $\text{NO}_3^-$  than the water into which it is mixing. For example, during the large flood wave of a hurricane, vertical

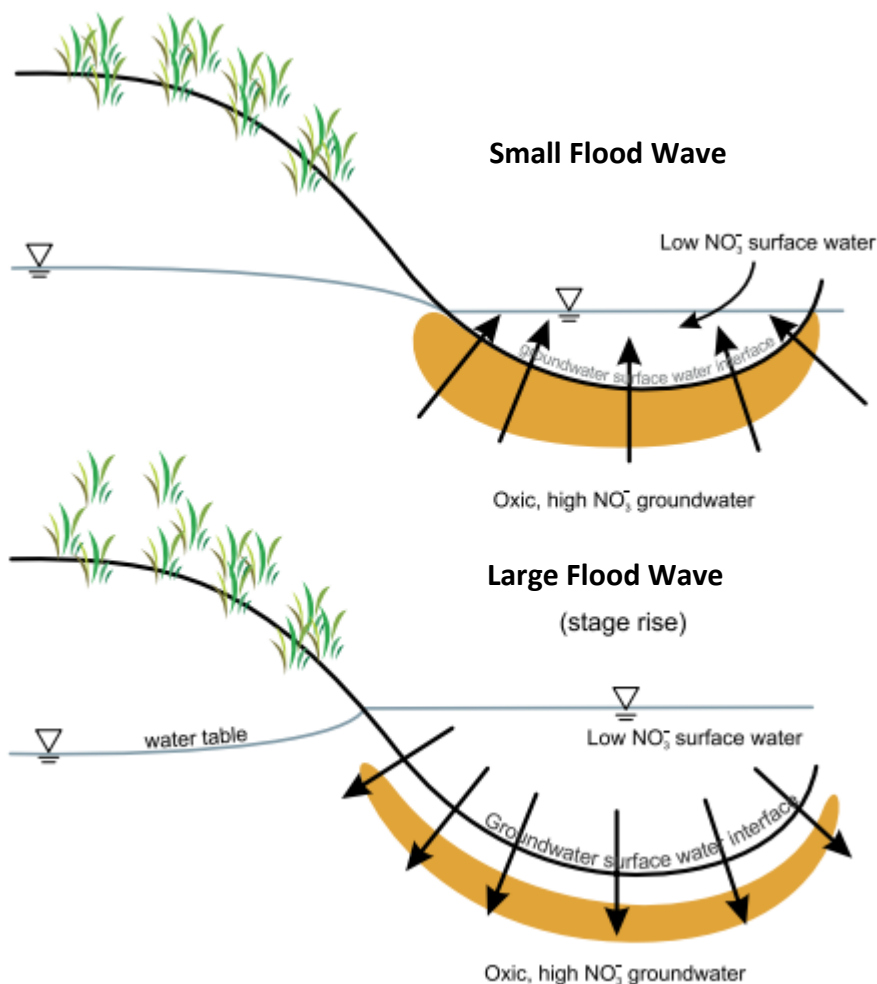


**Figure 1.1** Schematic illustration of the difference between large and small flood waves. In the top panel, a small flood wave creates a gradient toward up to the stream, result in groundwater discharge through denitrifying sediments indicated by the orange shaded area. In the bottom panel, the large flood wave allows the stage to rise above the water table, creating a gradient toward the streambed sediments. Flow is reversed, allowing oxygenated stream water to enter and inhibit the denitrification process. From [Gu *et al.* 2008]

infiltration in the floodplain aquifer and hyporheic zone can deliver oxygen-rich water to deeper sediments [Sawyer *et al.*, 2014]. Denitrification is inhibited by the oxygen during this recharge event. On the recession limb of the hydrograph, discharge from the groundwater to the stream could be enhanced over that during base flow, reducing the residence time of the water in the sediment, leading to lower residence times and less NO<sub>3</sub><sup>-</sup> removal. Thus, the flux during such a large storm might be higher than that observed during base flow [Gu *et al.*, 2008]. Similarly in

another study of a third-order stream in Southeast Pennsylvania during Hurricane Sandy (which occurred on Oct 2012), Sawyer et al. [2014] found that vertical infiltration during this large storm promoted the rapid rise of the water table and thus continuous groundwater discharge to the stream. This rapid hydraulic head response resulted in no bank storage of groundwater.

## 1.5 Objectives

Considering these various studies on the transient changes of hydraulic gradients, discharge, and nitrate concentrations during various sized storm events, the question this research addresses is: **How does storm intensity and duration affect nitrate flux as compared with base flow conditions?**

From October 2014 to February 2015, data from nine storms of various magnitudes and durations were collected at Cobb Mill Creek, VA. Water samples, precipitation data, and water elevations were used to describe each storm event captured. To measure the effect of storm intensity, precipitation intensity, flood wave size, and discharge were compared with the change in  $\text{NO}_3^-$  flux as compared to base flow conditions ( $\Delta J_{\text{NO}_3}$ ). To measure the effect of storm duration, storm duration and flood duration were compared with  $\Delta J_{\text{NO}_3}$ .

## Chapter 2. Methods

### 2.1 Sampling Location

This study was done at Cobb Mill Creek, located near Oyster, Virginia (Figure 2.1) on the property of the Anheuser-Busch Coastal Research Center. The coordinates of Cobb Mill Creek are a latitude of 37°17.485'N and a longitude of 75°55.868'N. Cobb Mill Creek drains an intensely cultivated region of unconsolidated, sandy Coastal Plain deposits [Mixon, 1985]. Cobb Mill Creek is a second-order, groundwater-dominated creek with strong evidence of vertical exchange and upwelling groundwater [Gu *et al.*, 2008; Mills *et al.*, 2011; Galavotti, 2004]. Like most streams on the Eastern Shore, Cobb Mill Creek has a forested riparian zone of varying thickness along most of its length. The portion of Cobb Mill Creek that was sampled has a relatively high slope (about 6 meters over a 200 meter distance) on one side of the bank and level ground on the other side. The creek drains through Oyster Harbor and Ship Shoal Channel to the Atlantic Ocean on the seaside of the Eastern Shore Peninsula.

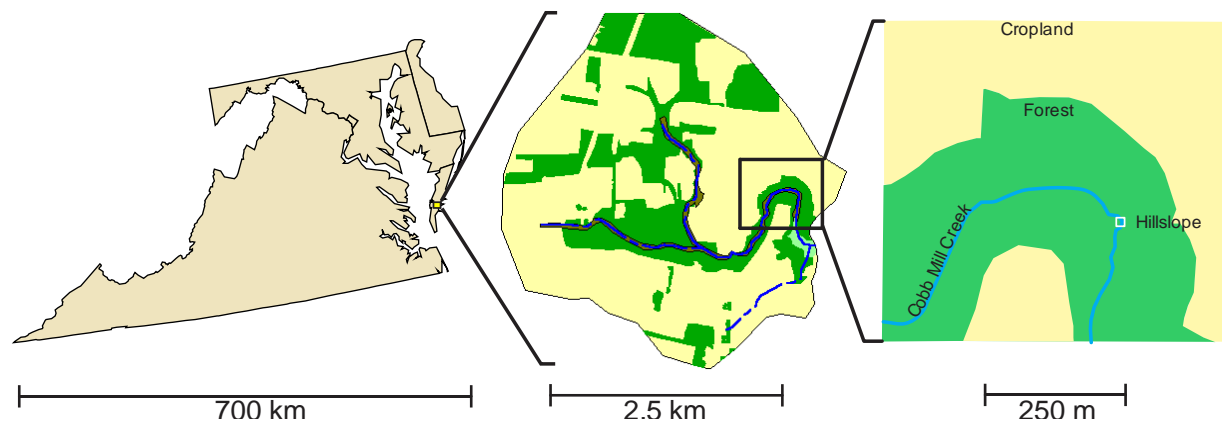


Figure 2.1. Location of Cobb Mill Creek in Virginia and the hillslope within the Cobb Mill Creek Watershed. Areas in green are forested.

## 2.2 Collection of Water Samples

Water samples for the determination of  $\text{NO}_3^-$  concentration were collected hourly during storm events using a stage-activated ISCO automatic sampler. The ISCO sampler comprised the level actuator, a pump, tubing, 24 collection bottles, a battery, and a programmable interface (Fig. 2.2). The level actuator was a way to trigger the sampler to start. When the tip of the sensor was wetted from the rising water level during a storm event, the sampler was triggered to collect 24 samples at 2-hour intervals. Between storms, the sensor was suspended 2.5 cm above the water level in the stream during base flow conditions. When a storm was predicted to be approaching, the sensor was lowered to about 1 cm in order to catch the very beginning of a storm. The sampling tube was attached at mid-depth in the stream to a length of rebar that was driven into

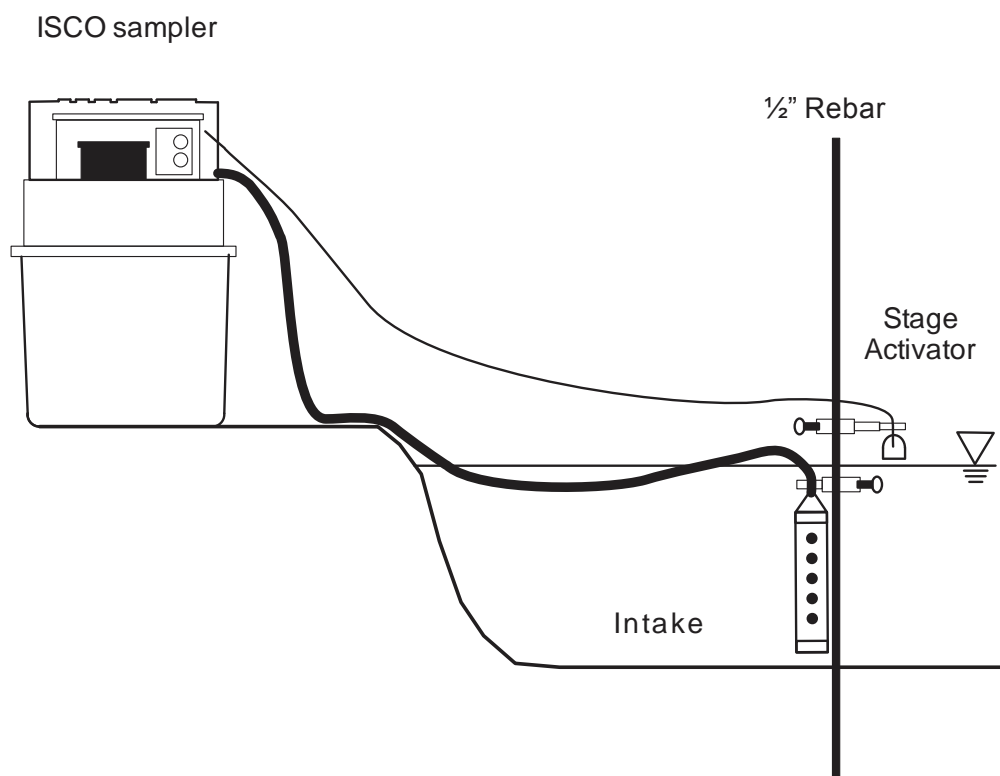


Fig 2.2 Schematic of the stage-activated automatic sampler for collecting stream water at regular intervals during storms.

the sediment. The rebar also held the stage activator at the water's surface. The rest of the equipment was placed on level ground on the stream bank. Two non-storm periods were sampled to compare base flow to storm conditions. In these cases, the ISCO collected hourly samples for 24 hours. Two base flow samples were taken prior to the November 1<sup>st</sup> storm and the February 9<sup>th</sup> storm.

### **2.3 Analysis of Water Samples**

Water samples were refrigerated upon collection and were returned to the laboratory in Charlottesville to be filtered. Most water samples were filtered within two weeks to prevent the biodegradation of water samples. However, for the November 1<sup>st</sup> storm, samples 9 through 13 (captured on November 2 at 7:58 through 15:58) were filtered three weeks later because there was a delay in delivery from the Eastern Shore field station to the lab in Charlottesville.

Once filtered, concentration of  $\text{NO}_3^-$  in the collected water samples was analyzed by ion chromatography (IC) using a Dionex Ion Chromatograph ICS-2100. An automated sampler (Dionex AS-DV) was connected to the IC for 50-sample batch processing. The sample sequences used to run the IC and autosampler were programmed using the Chromeleon Software version 6.8. The IC was programmed to run at a column temperature of 35°C, 1 mL min<sup>-1</sup> flow rate, 34 mM KOH eluent concentration, 90 mA suppressor current, and a runtime of 15 minutes. The column was a 4-mm Dionex AS18. Each water sample was analyzed once. Samples were run in chronological order of collection, and if the concentration values obtained looked like outliers and not within 2 ppm of the neighboring values, then the samples were reanalyzed with the IC.

Nitrate concentrations were then converted to nitrogen measurements to determine how much nitrogen was present in the water sample. Using nitrate and elemental nitrogen's

molar mass,  $62 \text{ g mol}^{-1}$  and  $14 \text{ g mol}^{-1}$  respectively, it was determined that  $14/62$  or 0.226% of nitrate was made up of nitrogen. All nitrate concentrations for the water samples were then multiplied by 0.226 to determine nitrogen concentrations. Thus, for the remainder of this thesis, all nitrate values are expressed as nitrogen.

## **2.4 Determination of Combined Hydrograph and Hyetograph**

### **2.4.1 Stream stage**

A submerged Levellogger® pressure transducer (Solinst) was used to determine the stream stage. Pressure readings were corrected for changing air pressure by a second transducer (Solinst Barologger®) hung in the air above the water surface. Both transducers were hung vertically in a stilling well on the creek bank and connected to the stream by a flexible tube which terminated inside a section of 2-inch diameter, 0.1-inch slotted well screen driven into the sediment. The well screen served to keep sediment from clogging the opening of the tubing. Both transducers collected a pressure measurement every 6 minutes and the data was downloaded to a laptop computer every two to four months. The change in water level was calculated by subtracting the barometric pressure from the total pressure measured by the stream transducer (the transducer output has units of meters of water). The initial stream level was calculated by subtracting the MSL elevation at the top of the stilling well with the depth from the lip of the stilling well to the top of the water surface. With the change in water level for every 6 minutes and the initial stream level, a continuous stage hydrograph of Cobb Mill Creek was produced.

During the September sampling period, the barometric pressure transducer at Cobb Mill Creek failed, so a regression was computed between the North Shore barometer and Cobb Mill Creek's barometer (Eqn. 1). The North Shore barometer was also located 12.6 miles (20km)

away from Cobb Mill Creek's barometer, just south of the town of Nassawadox. Since there was no barometric pressure reading at Cobb Mill Creek, the North Shore barometer provided the barometric data needed. With an  $r^2$  value of 0.9739, the September North Shore barometer readings were used to reasonably approximate barometer readings at Cobb Mill Creek through the following equation:

$$\text{Cobb Mill Creek Barometer} = 1.0086 \times \text{North Shore Barometer} - 0.0224, \quad r^2=0.9739 \quad (1)$$

At the Cobb Mill Creek site, there were two pressure transducers already installed. One transducer was in the stilling well where the majority of pressure readings were utilized. The other transducer was by a culvert, located 220 meters upstream of the stilling well. During the July sampling period when Cobb Mill Creek's pressure transducer in the stilling well failed to collect data, another regression was computed using the relationship between already obtained pressure readings at Cobb Mill Creek's culvert and at the stilling well. With this close proximity to the stilling well and a high  $r^2$  value of 0.9709 (Eqn. 2), the pressure readings at the culvert provide a reasonable estimation for the stilling well. Using the July pressure readings at the nearby culvert, estimated pressure readings at the sampling site were calculated using the following equation:

$$\text{Stilling Well Pressure} = 0.8782 \times (\text{Culvert Pressure}) + 0.2798, \quad r^2= 0.9709 \quad (2)$$

These calculated pressure readings were then converted into stream stage in the previously mentioned compensation method.

## 2.4.2 Precipitation

Precipitation records for each storm event were taken from a precipitation gauge at a station monitored by the National Oceanic and Atmospheric Administration (NOAA), 200 m

away from Cobb Mill Creek where the water samples were taken [Sofranko, 2007]. The precipitation data were reported in millimeters of rainfall per hour and were available online under the site location name of “VA Cape Charles 5 ENE: Anheuser Busch Coastal Res. Ctr. Univ. of VA (Oyster)” at

[http://www.ncdc.noaa.gov/crn/report?report=newelements&network=&por\\_start\\_month=01&por\\_start\\_day=01&por\\_start\\_year=2013&por\\_start\\_hour=&por\\_end\\_month=&por\\_end\\_day=&por\\_end\\_year=&por\\_end\\_hour=&por\\_tref=LST&sort\\_by=slv&comm\\_only=&flags=0&elements=&element\\_group\\_id=&format=web](http://www.ncdc.noaa.gov/crn/report?report=newelements&network=&por_start_month=01&por_start_day=01&por_start_year=2013&por_start_hour=&por_end_month=&por_end_day=&por_end_year=&por_end_hour=&por_tref=LST&sort_by=slv&comm_only=&flags=0&elements=&element_group_id=&format=web).

## 2.5 Determining Change in Discharge and Nitrate Flux

In order to determine discharge during base flow and during the storm event, the continuous stage measurements were converted to discharge measurements using a predetermined discharge rating curve for Cobb Mill Creek at the culvert [Pickus *et al.*, 2014] (Figure 2.3) (Eqn. 3):

$$Q = (9.67 \times 10^{-5}) \times Stage^{14.8} \quad (3)$$

The culvert gauging point is 220 meters upstream from the gauge at the hillslope. The continuity assumption asserts that discharge at the culvert would be the same at the sampling site with no significant water loss or gain. The sum of the coefficients in Equation 2 was almost equivalent to 1, which means that the data collected at the culvert are translatable to the hillslope stilling well. Along with the high  $r^2$  (Eqn. 2), this equation suggests that with the minor adjustments in the culvert discharge, the adjusted value is a reasonable approximation of discharge at the hillslope.

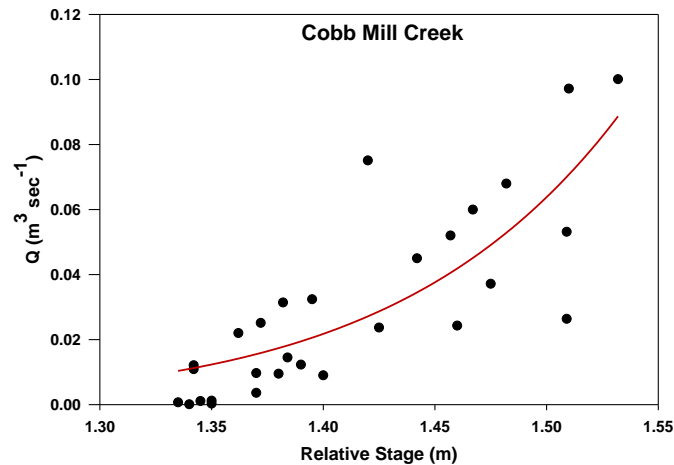


**Figure 2.3.** Rating curve for the culvert gauge at Cobb Mill Creek. (Pickus *et al.*, 2014)

Discharge ( $Q$ ) was used in conjunction with the  $\text{NO}_3^-$  concentration ( $C$ ) to calculate  $\text{NO}_3^-$  flux ( $J$ ) by multiplying discharge by concentration:

$$J [\text{M} \cdot \text{T}^{-1}] = C[\text{M} \cdot \text{V}] \times Q[\text{V} \cdot \text{T}^{-1}] \quad (4)$$

where  $T$  represents the duration of the flood wave.

The discharge measurements within every hour were summed up to determine hourly discharge. These hourly discharge measurements were then multiplied by the corresponding average nitrate concentrations to calculate flux for that hour. By adding together the hourly fluxes for a storm, the flux over the duration of the storm was determined.

## 2.6 Hydraulic Gradients

In order to understand how storms affect near-stream hydraulic gradients, two wells were installed in the stream bank and the adjacent hillslope with Levellogger® pressure transducers. The stream bank well was 0.5m away from the stream and the hillslope well was 10.0m away from the stream. Using the pressure transducers installed in the wells, the water table elevations were calculated the same way stream stage was calculated from the pressure readings in the

stilling well. Hydraulic gradients were then calculated using the water table elevations in the wells penetrating the stream bank and stream surface elevations in the stilling well. Water table elevations were subtracted from the stream stage and then divided by the distance between them.

## 2.7 Storm Intensity and Duration

In order to determine how storm intensity and duration affected nitrate concentrations in the stream, the change in nitrogen flux ( $\Delta J_{\text{NO}_3}$ ) of each storm was compared with different parameters during a storm. The  $\Delta J_{\text{NO}_3}$  was determined as

$$\Delta J_{\text{NO}_3} = \text{NO}_3^- \text{ flux during storm} - \text{NO}_3^- \text{ flux at base flow.} \quad (5)$$

Negative values of  $\Delta J_{\text{NO}_3}$  indicate that less  $\text{NO}_3^-$  was moved in the stream discharge during a storm than in the immediately antecedent base flow period. If a base flow sample was not taken during the storm event, then the first sample of the storm event was used for the base flow nitrogen concentration because the first was the closest water sample to base flow.

In order to determine how storm intensity affected  $\text{NO}_3^-$  fluxes, the change in  $\text{NO}_3^-$  flux ( $\Delta J_{\text{NO}_3}$ ) was plotted against various storm characteristics including total precipitation, peak hourly intensity of rainfall, flood wave height and water flux. In order to observe how the duration of a storm affected nitrate concentration in the stream, the time it took a flood wave to pass was plotted against the change in nitrate flux. The total hours of precipitation was also plotted against change in nitrate flux. Pearson's  $r$  values were then calculated to compare the strengths of the correlations between  $\Delta J_{\text{NO}_3}$  and these storm parameters.

## Chapter 3. Results

### 3.1 Summary of Storm Events Captured

Nine storm events were captured between October 22, 2014 and February 9, 2014, and a summary of those events is located in Table 3.1. Storm duration was determined as the number of hours in which precipitation was recorded. Some storms (December 24<sup>th</sup>, December 29<sup>th</sup>, January 12<sup>th</sup>, February 2<sup>nd</sup>, and February 9<sup>th</sup>) did not have continuous rainfall. There were breaks in the rainfall that spanned from 1 hour to 5 hours. These breaks were considered as part of the storm duration because the stream stage never returned to base flow during the break. The storm starting January 12, 2015 had a large, 21-hour break between two rainfall sessions. However, because the stage did not return to base flow during the 21-hour break, the two rainfall sessions were counted as one storm event and the storm duration was reported as 52 hours and included the break (Table 3.1). Storm duration ranged from 3 hours to 52 hours.

Flood duration was the duration (i.e., width of the peak on the time axis) of the flood wave and ranged from 4.00 hours to 126 hours. Total precipitation during the various storm events was the sum of the hourly precipitation during the event, and ranged from 1.71mm to 36.7mm. Peak hourly intensity was the total precipitation divided by the total hours of precipitation. For intensity calculations, breaks in the rainfall were not counted in the total hours of precipitation. Peak hourly intensity ranged from 0.542 mm h<sup>-1</sup> to 6.11mm h<sup>-1</sup>. Flood wave height was the difference between the peak stage in the flood wave and the stage at base flow immediately preceding the flood. Flood waves ranged from 3.60cm to 21.5cm. Change in discharge ( $\Delta Q$ ) was the difference between the total water flux during the storm and for a similar time period under the base flow conditions immediately preceding the flood.  $\Delta Q$  ranged from -0.569 m<sup>3</sup> to 29,900 m<sup>3</sup>. The final parameter was change in nitrate flux ( $\Delta J_{NO_3}$ ) which was

defined as the difference between total nitrate flux during the storm and total nitrate flux during the base flow period of the same duration as the storm but prior to the storm. Change in flux ranged from -0.00909kg to 36.0kg.

**Table 1.** Summary of storm events

Date	Storm Duration <sup>a</sup> (h)	Flood Duration (h)	Total Precipitation (mm)	Peak Hourly Intensity (mm h <sup>-1</sup> )	Flood wave height (cm)	$\Delta Q$ (m <sup>3</sup> )	$\Delta J_{NO_3^-}$ (kg)
10/22/14-10/23/14	6	25.0	16.1	2.68	7.54	22.9	-0.00909
11/01/14-11/03/14	4	4.00	2.17	0.542	3.60	-0.569	-0.00238
11/17/14-11/19/14	6	36.7	36.7	6.11	21.3	842	0.454
12/25/14-12/26/14	19	60.1	34.8	2.49	21.5	29,900	32.6
12/29/14-12/31/14	11	50.9	14.1	1.41	7.92	12,000	18.0
1/12/15-1/14/15	52	126	32.5	1.16	17.6	10,500	18.0
1/18/15-1/20/15	4	96.6	21.3	5.32	16.2	20,300	36.0
2/2/15-2/3/15	3	d	1.71	0.571	d	d	d
2/9/15-2/11/15	12	d	3.27	0.546	d	d	d

<sup>a</sup>Number of hours of active rainfall.

<sup>b</sup>Number of hours during which the hydrograph was above base flow.

<sup>c</sup>Difference between the N flux during the storm, and the N flux for a period of the same duration during base flow.

<sup>d</sup>February storms were so small that no flood wave was discernable in the stage hydrograph (Figure 3.8 and 3.9).

The flood duration, change in stage, change in discharge and change in nitrate flux could not be calculated.

### 3.2 Stream Stage, Nitrate Concentration, and Precipitation

The precipitation recorded in the 9 events ranged in magnitude from very small (1.71 mm) to moderate (36.7 mm) with no major storms such as hurricanes occurring during that time period (Table 3.1). The hyetograph, stage hydrograph, and  $NO_3^-$  concentrations in the collected water samples were plotted for each of the nine storm events (Figure 3.1-3.9). For the two non-

storm events, only the hydrograph and nitrate concentrations were plotted (Figure 3.10-3.11). Data from the pressure transducers were converted to stream stage as described in the Methods section and then plotted in units of meters above mean sea level (MASL). Nitrate concentrations are expressed as nitrate-nitrogen ( $\text{NO}_3^-$ -N) and plotted in units of  $\text{mg L}^{-1}$ . Precipitation data obtained from NOAA records were plotted in millimeters on a reverse y-axis.

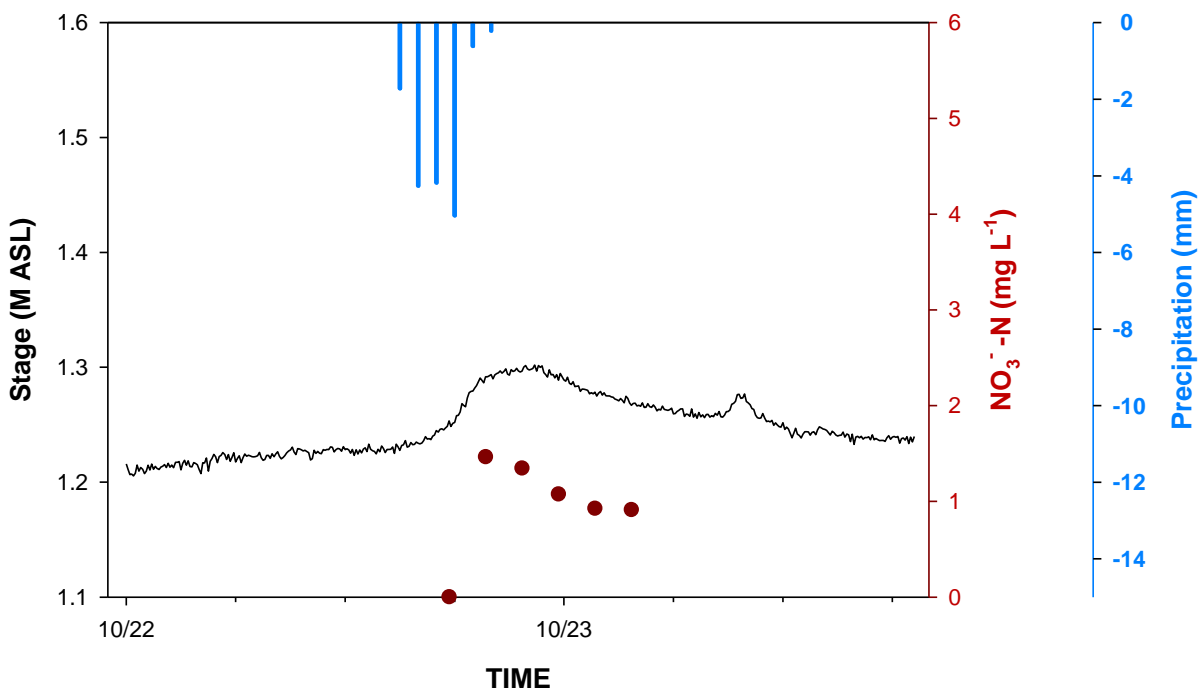


**Figure 3.1.** Precipitation, stream stage, and  $\text{NO}_3^-$ -N concentration in hourly samples for a storm starting on October 22, 2014. Although the sampler was intended to collect 24 samples over a 48-hr period, the distributor arm jammed such that only 6 samples were collected.

The automatic sampler was set to collect 24 water samples spanning a 48-hour period, however, occasional problems arose that resulted in a loss of some samples. The storms that occurred on October 22<sup>nd</sup> and February 2<sup>nd</sup> collected fewer samples due to a jammed distributor arm in the automatic sampler (Figure 3.1 and 3.8). In these cases, the distributor could not rotate to the next sample bottle.

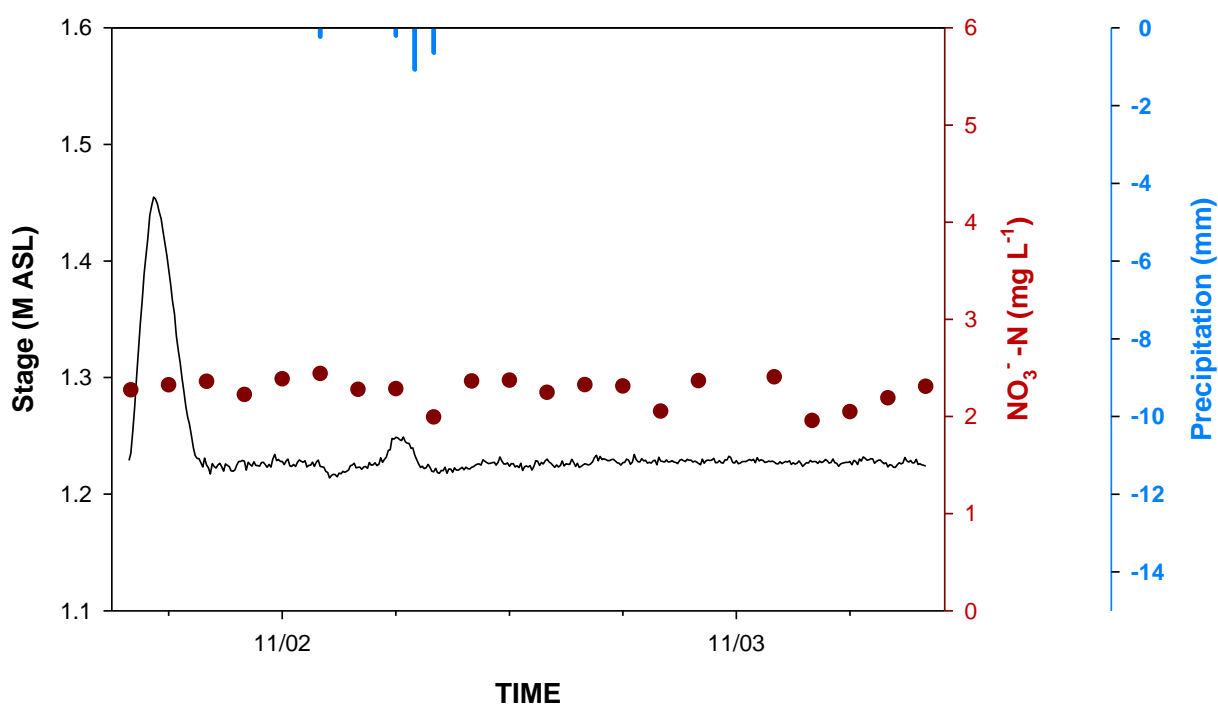


**Figure 3.2.** Precipitation, stream stage, and NO<sub>3</sub><sup>-</sup>-N concentration in hourly samples for a storm that started on November 1, 2014. The initial peak that represents a change in stage of 23 cm was not related to any storm, and cannot be explained. The flood wave resulting from the rainfall on Nov. 2 is much smaller and in proportion with the amount of rain that fell. The sample captured on November 3 at midnight was never received at the laboratory and therefore is missing from the plot of the NO<sub>3</sub><sup>-</sup> data.

In general, nitrate concentrations decreased during the passing of a flood wave. For the storms with discernible flood waves, nitrate concentrations decreased to their lowest levels shortly after the peak of the flood wave and then steadily increased as the wave receded. During the storm on November 17, the nitrate concentration decreased from 1.10mg L<sup>-1</sup> at base flow to 0.267mg L<sup>-1</sup> during the passage of the flood wave (Figure 3.3). For storms with two flood waves

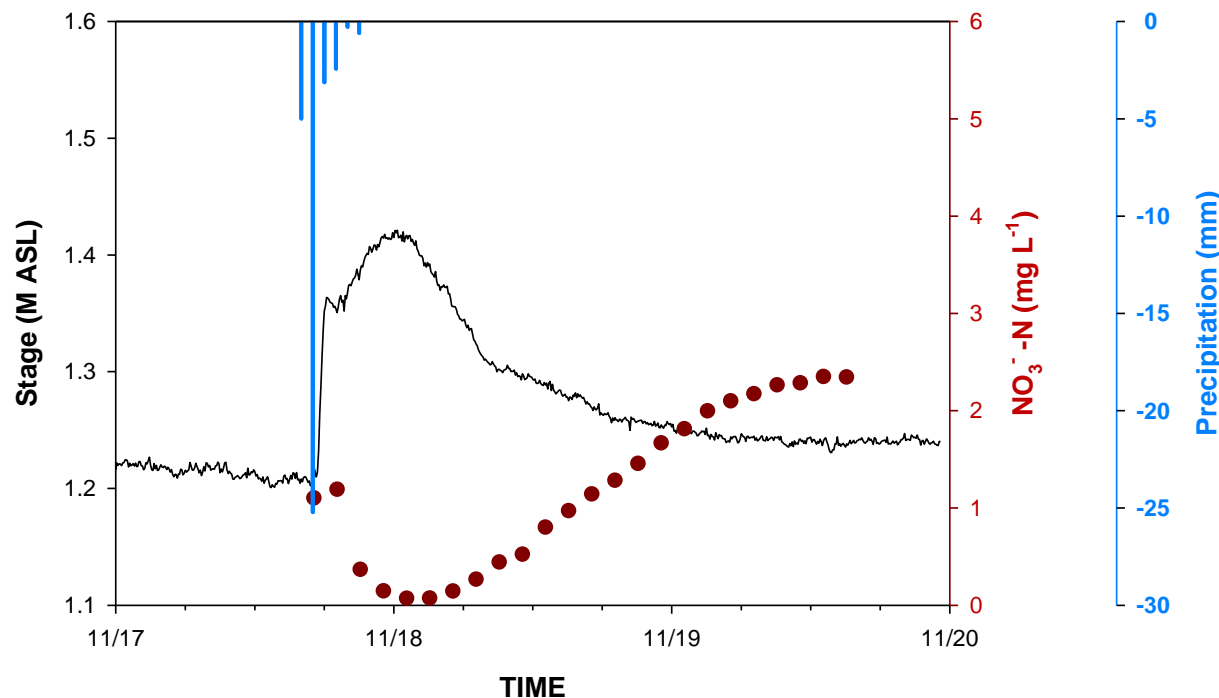


**Figure 3.3.** Precipitation, stream stage, and  $\text{NO}_3^-$ -N concentration in hourly samples for a storm that started on November 17, 2014.

(Figure 3.4 and 3.6), nitrate concentrations exhibited similar patterns of decreasing nitrate, but the concentration decreased twice with each passing flood wave. For storms with small flood waves of 7.54cm or smaller, nitrate concentration patterns behaved differently. During the October 23<sup>rd</sup> storm (Figure 3.1), nitrate was highest ( $1.46\text{mg L}^{-1}$ ) at the peak of the flood wave but then decreased to  $0.913\text{mg L}^{-1}$  as the discharge returned to base flow after passage of a small flood wave of 7.54cm. For storms with indistinguishable flood waves (Figure 3.8 and 3.9), there were no changes in nitrate concentrations. The February storms had low total precipitation (1.71mm and 3.27mm) and low peak hourly intensities ( $0.571\text{mm h}^{-1}$  and  $0.546\text{mm h}^{-1}$ ).

During the non-storm event starting on July 11<sup>th</sup>, the pattern of nitrate concentrations was sinusoidal in shape (Figure 3.10). During the non-storm event starting on September 27<sup>th</sup>, there were no changes in nitrate concentration in the collected samples.

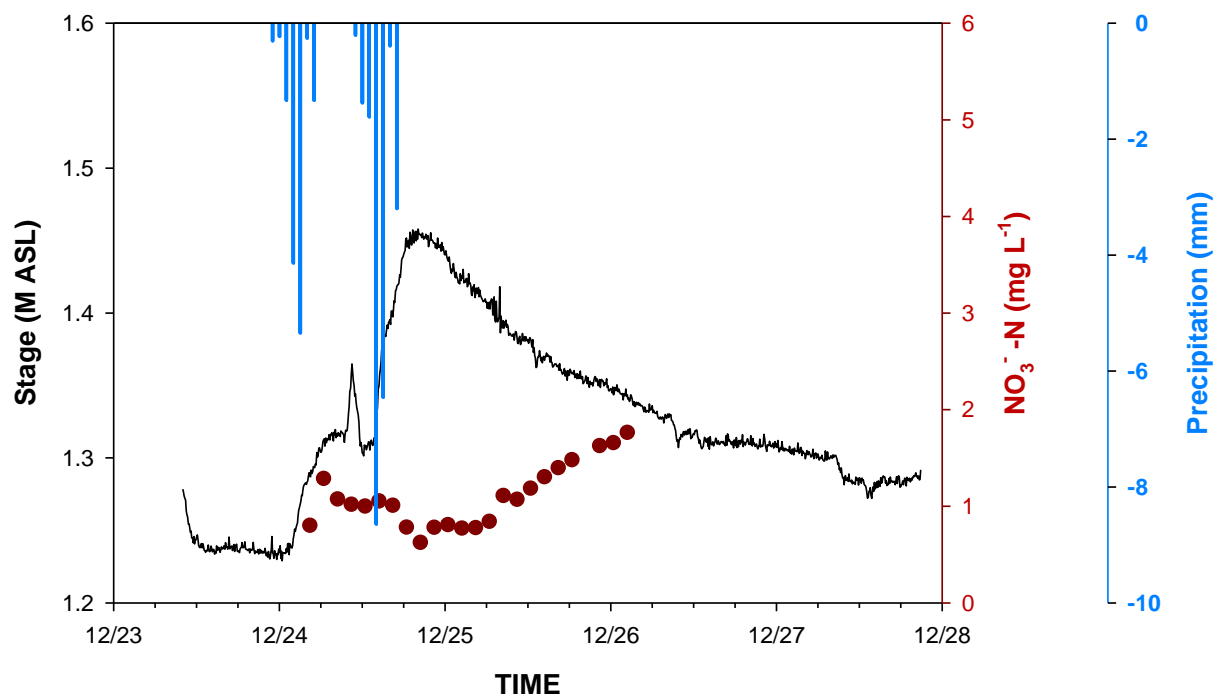


**Figure 3.4.** Precipitation, stream stage, and  $\text{NO}_3^-$ -N concentration in hourly samples for a storm that started on December 24, 2014

One irregularity that occurred in most of the sampled events (July 11<sup>th</sup>, September 27<sup>th</sup>, October 23<sup>rd</sup>, December 24<sup>th</sup>, December 28<sup>th</sup>, January 12<sup>th</sup>, February 2<sup>nd</sup>, February 8<sup>th</sup>) was that the  $\text{NO}_3^-$  concentration in the first water sample collected was relatively low compared to that in the rest of the samples. The irregularity cannot be explained; however, these concentrations, near  $0\text{mg L}^{-1}$ , could have resulted from problems with the automatic sampler.

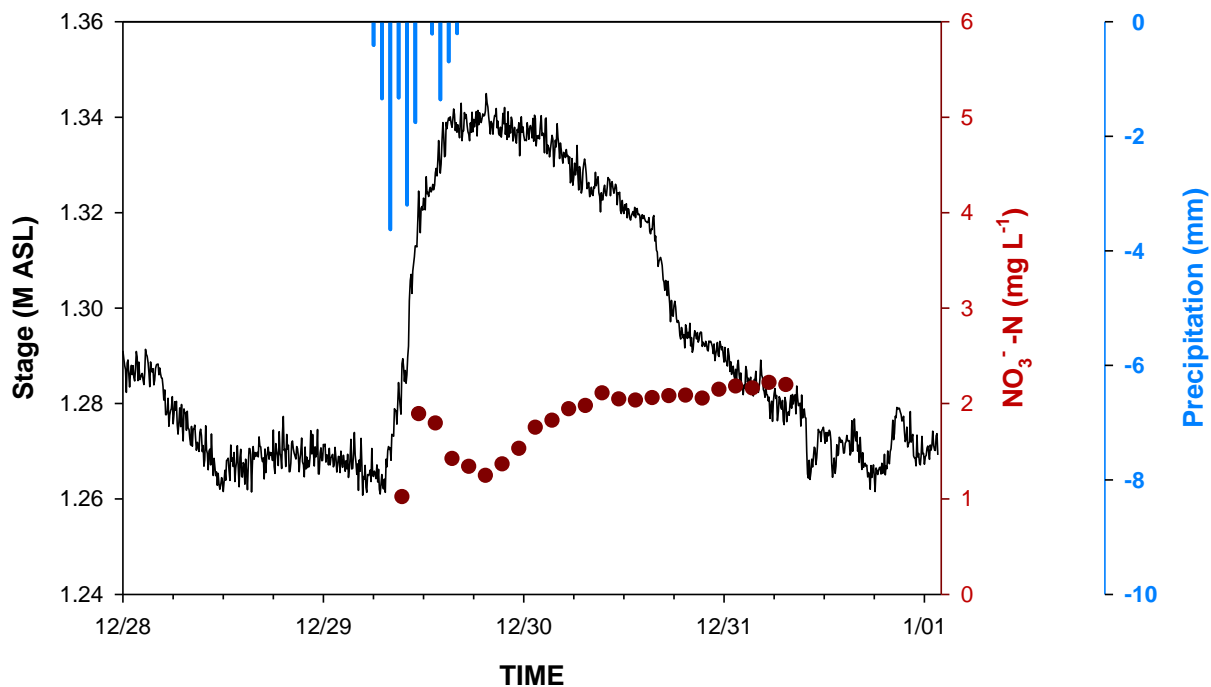


**Figure 3.5.** Precipitation, stream stage, and  $\text{NO}_3^-$ -N concentration in hourly samples for a storm starting on December 29, 2014

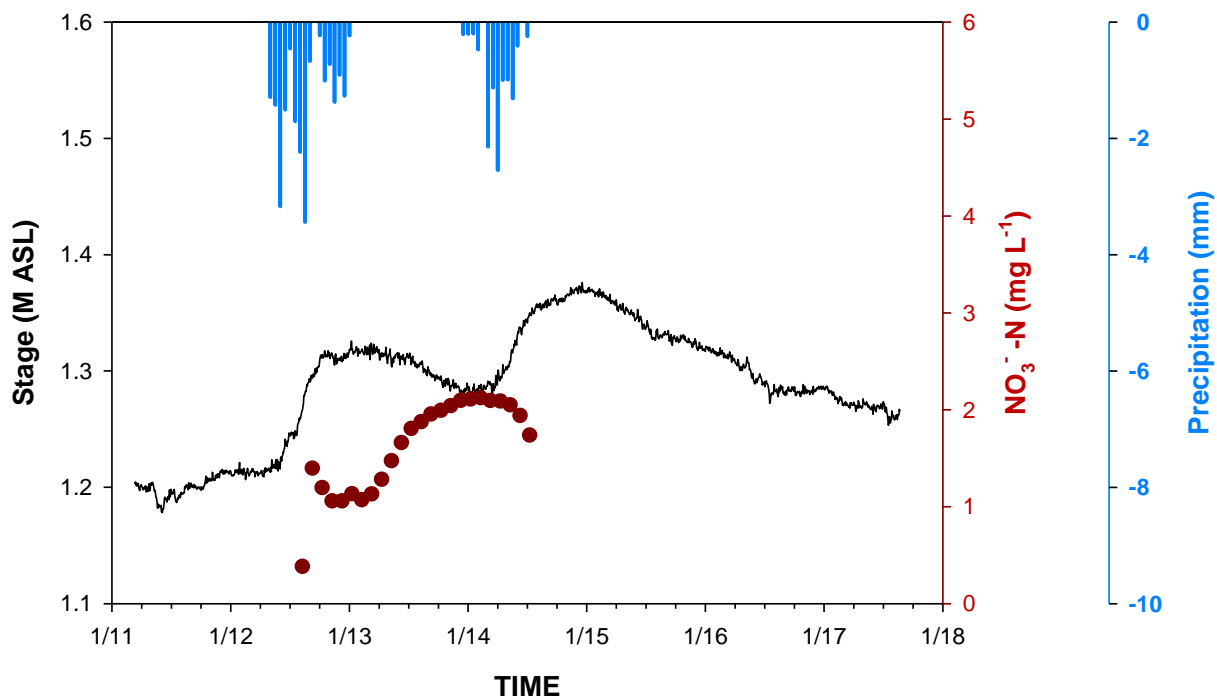


**Figure 3.6.** Precipitation, stream stage, and  $\text{NO}_3^-$ -N concentration in hourly samples for a storm starting on January 12, 2015

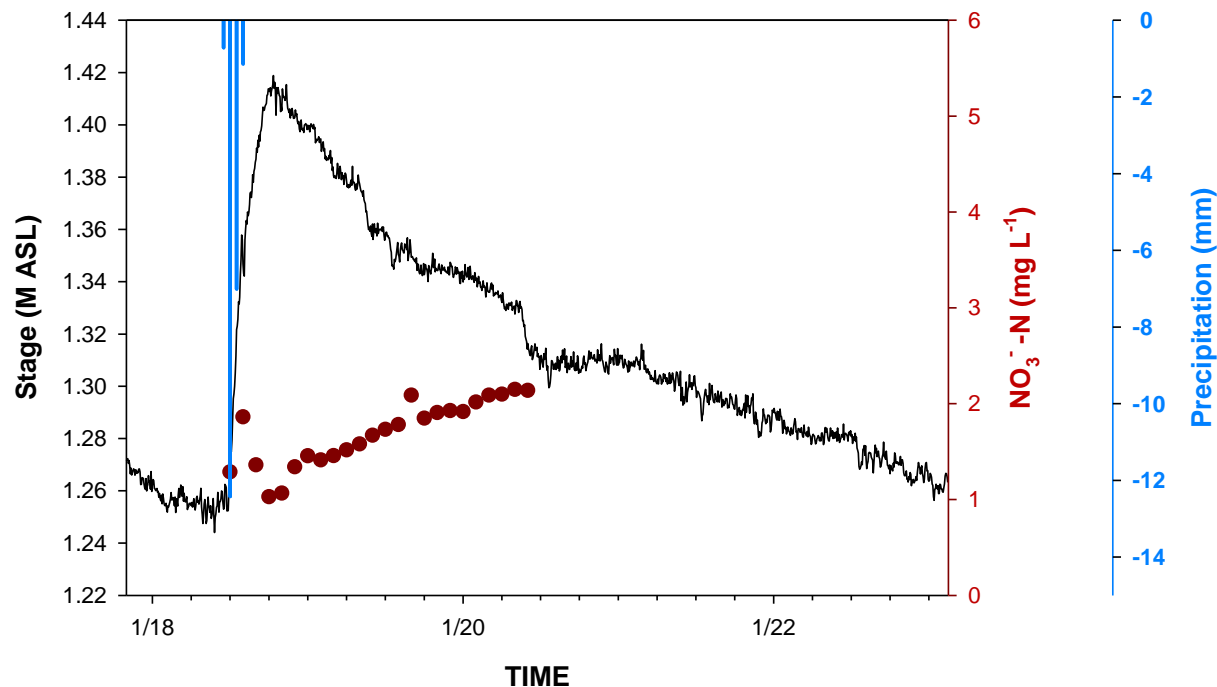


**Figure 3.7.** Precipitation, stream stage, and NO<sub>3</sub><sup>-</sup>-N concentration in hourly samples for a storm starting on January 18, 2015

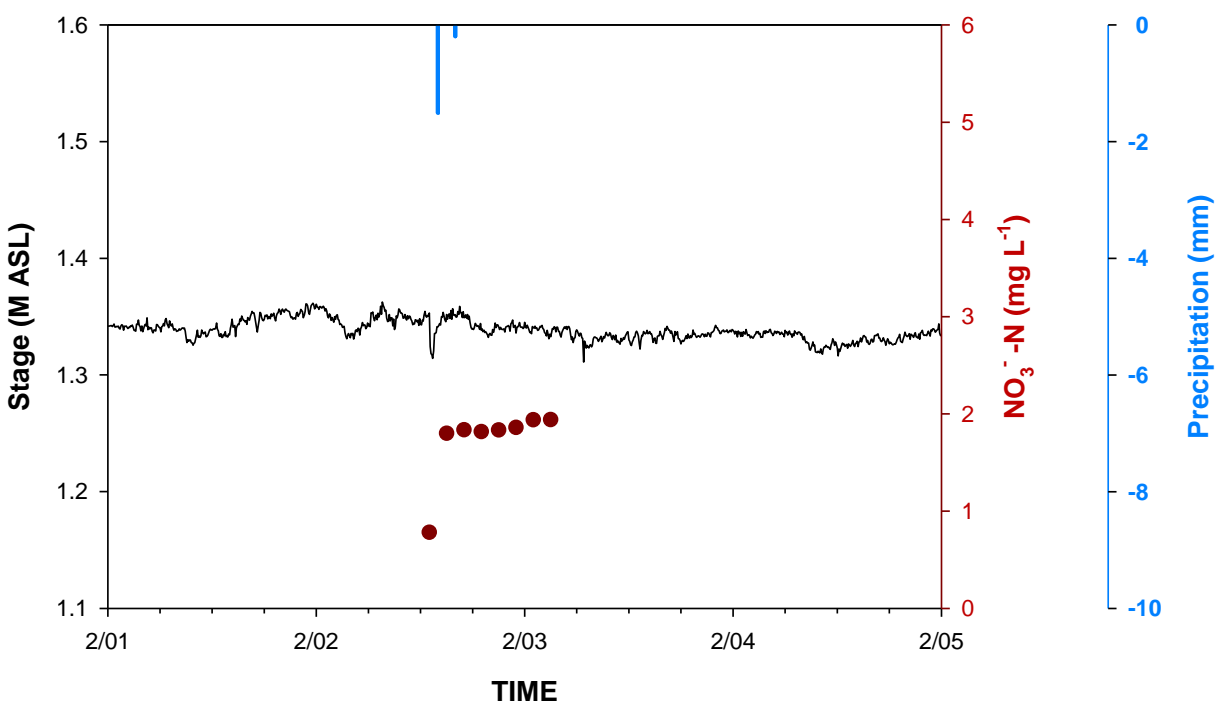


**Figure 3.8.** Precipitation, stream stage, and NO<sub>3</sub><sup>-</sup>-N concentration in hourly samples for a storm starting on February 2, 2015. Although the sampler was intended to collect 24 samples over a 48-hr period, the distributor arm jammed such that only 8 samples were collected.

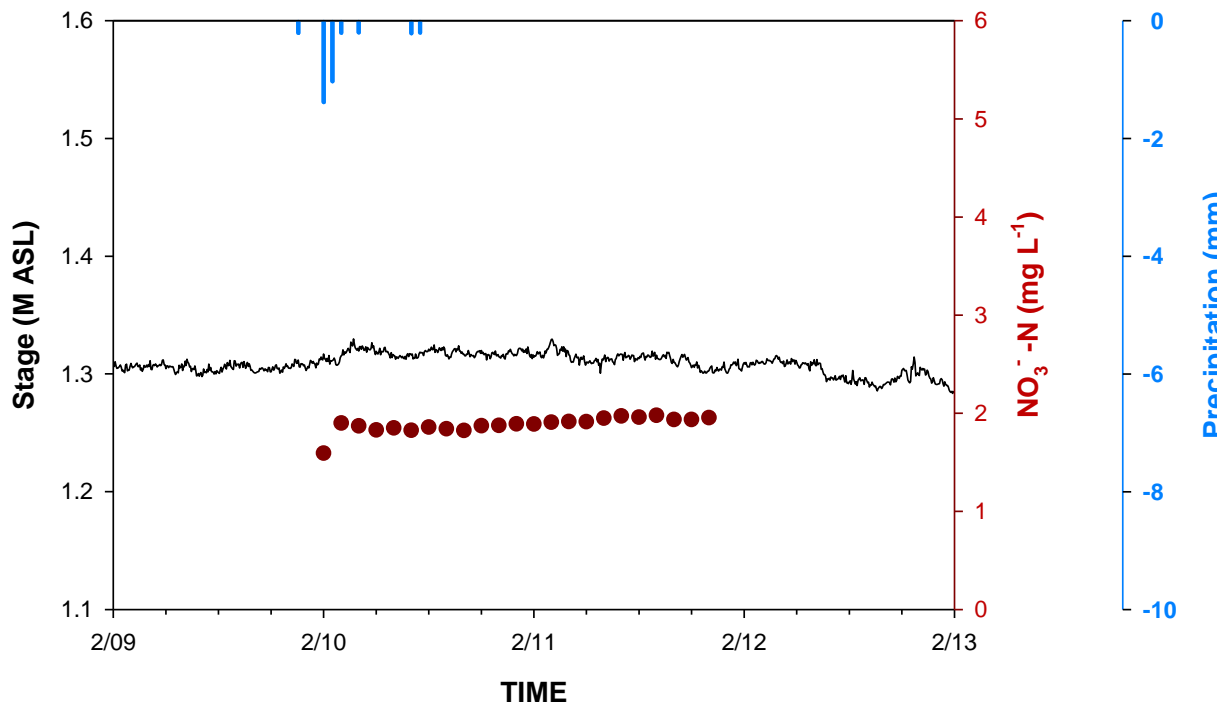


**Figure 3.9.** Precipitation, stream stage, and  $\text{NO}_3^-$ -N concentration in hourly samples for a storm starting on February 9, 2015. Although the sampler was intended to collect 24 samples over a 48-hr period, only 23 samples were collected for some unknown reason.

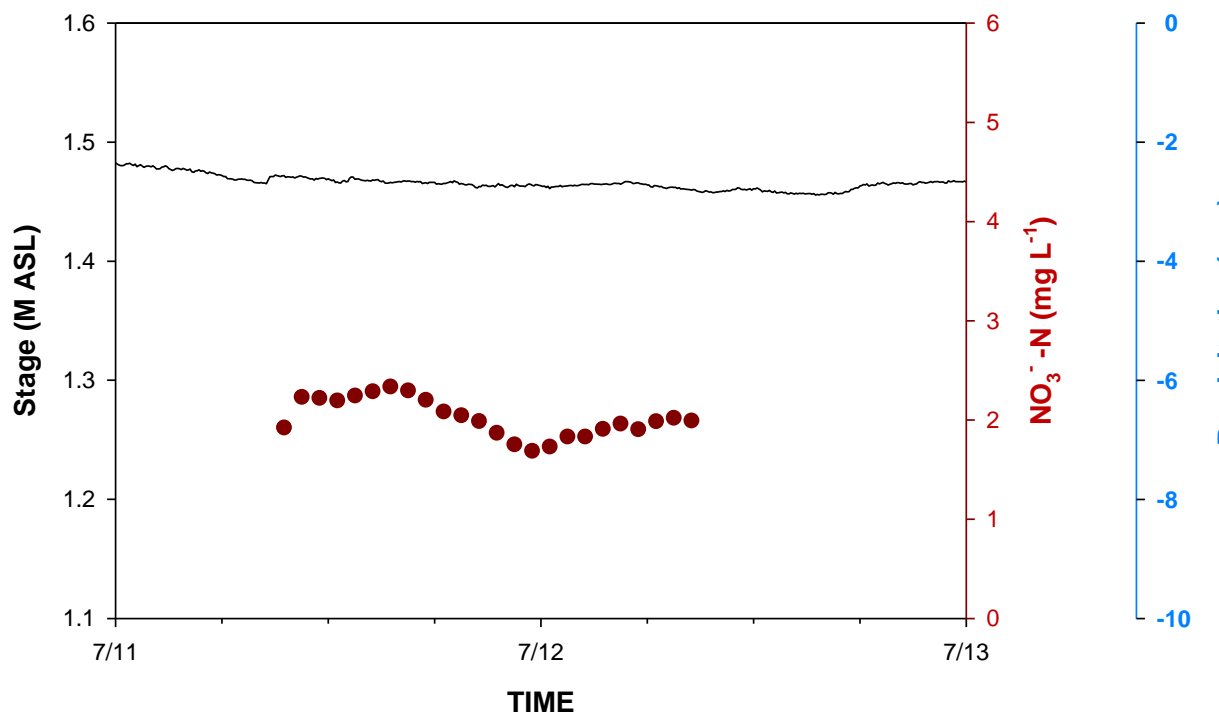


**Figure 3.10.** Precipitation, stream stage, and  $\text{NO}_3^-$ -N concentrations for a non-storm event on July 11, 2014. The precipitation axis is included, but there was no rainfall during the indicated period.

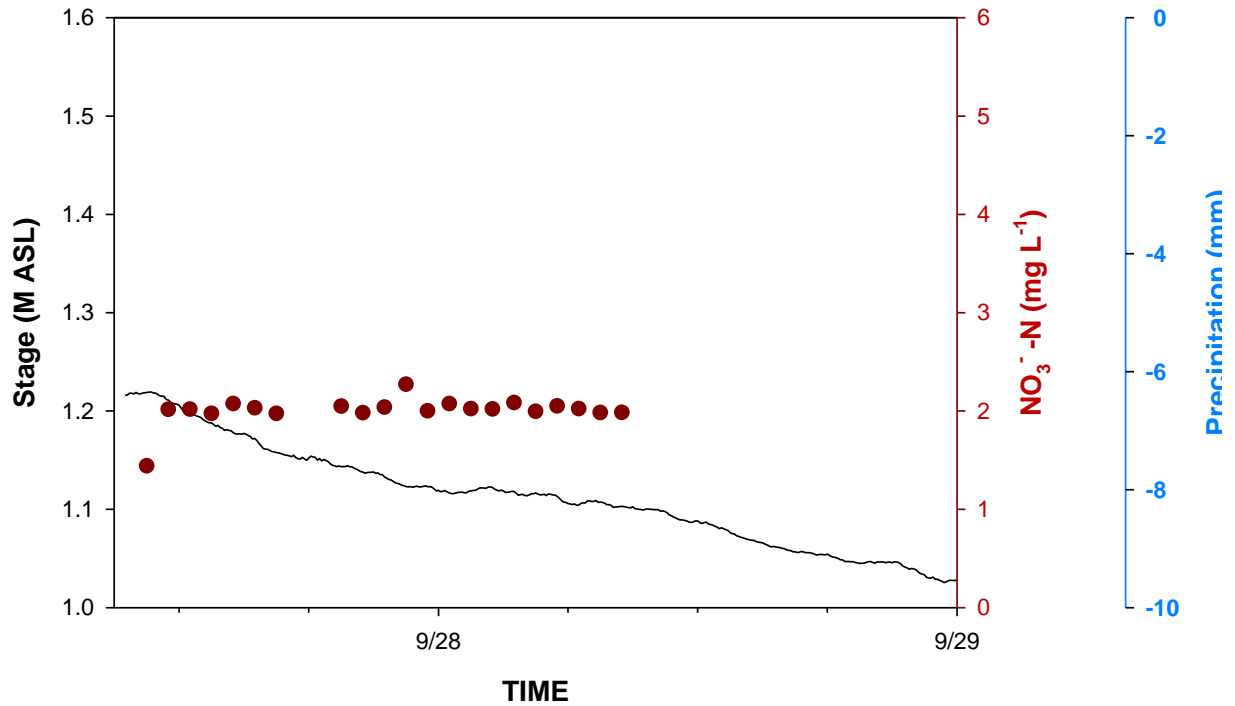


**Figure 3.11.** Precipitation, stream stage, and  $\text{NO}_3^-$ -N concentrations for a non-storm event on September 27, 2014. The precipitation axis is included, but there was no rainfall during the indicated period.

### 3.3 Head Gradients

The hydraulic gradient is the difference between the water table elevation in the stream bank and the stream stage divided by 0.5 meters, the horizontal distance between the two measuring wells. Data from the pressure transducers in the stream bank well and hillslope were converted to water table elevation values. When plotted, the water table elevations in the hillslope showed no major fluctuations in relation to the stream stage. As a result, only the head gradient between the water table elevation at the stream bank and stream stage were calculated and plotted. Only three storms were graphed (Figure 3.12-3.15) because the pressure transducer in the stream bank well failed to collect data past the November 17<sup>th</sup> storm.

For each storm, the water table elevation in the stream bank was always higher than the stream stage and mimicked every action in the stream stage. However the head gradients

responded differently to each storm. During the November 17<sup>th</sup> storm, the head gradient increased sharply at the beginning of the flood wave, jumping from 0.2 to 0.4 (Figure 3.14) because of a high intense rainfall of 36.7mm at a peak hourly intensity of 6.11mm h<sup>-1</sup> (Table 3.1). During the November 1<sup>st</sup> storm, hydraulic gradient increased slightly from 0.09 to 0.16 (Figure 3.13). There was only 2.17mm of rain falling at a peak hourly intensity of 0.542. Lastly, the October 22, 2014 storm exhibited no discernible changes in the head gradient (Figure 3.12). While rainfall and peak hourly intensity was higher than the November 1<sup>st</sup> storm, there were no discernible changes in gradient because the flood wave was uniquely longer and barely discernible. As a result, the change in head gradient was even more minute.

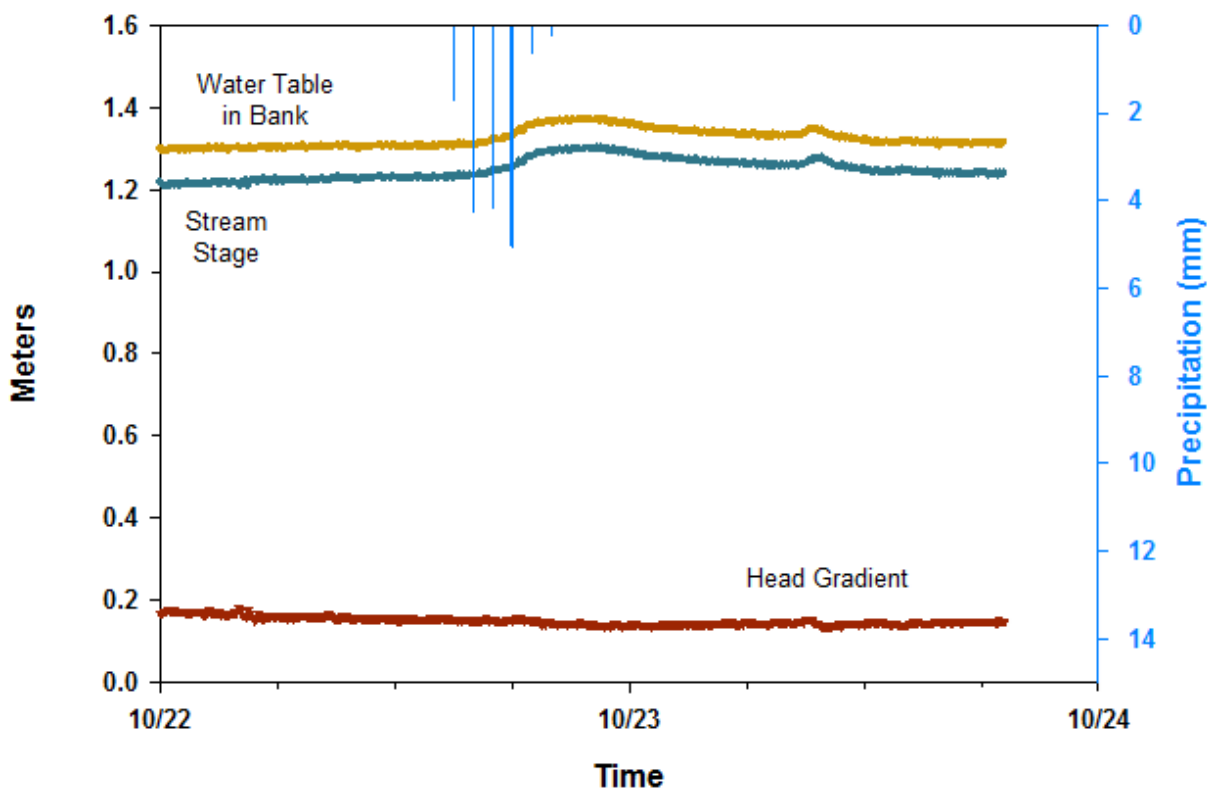


**Figure 3.12.** Precipitation, stream stage, water table elevation and head gradient during storm starting October 22, 2014

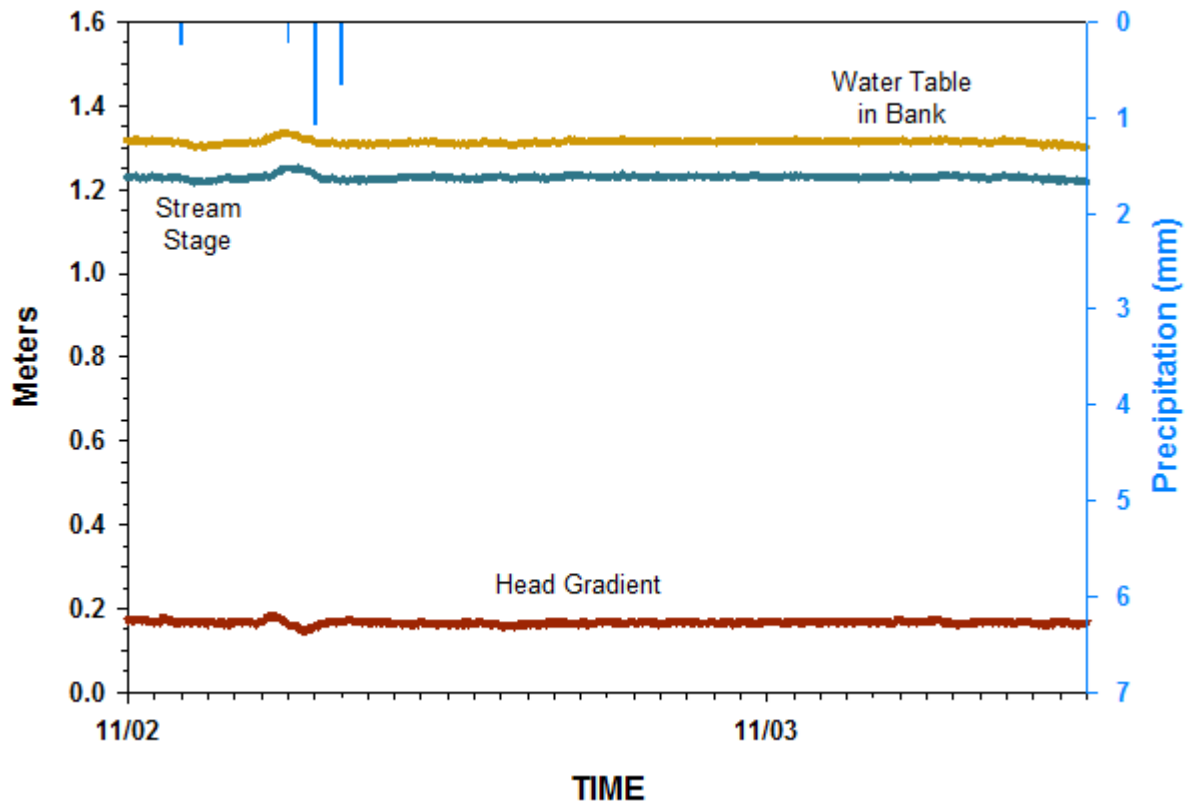


**Figure 3.13.** Stream stage, water table elevation and head gradient during storm starting November 1, 2014. The initial peak that represents a change in stage of 23 cm was not related to any storm, and cannot be explained.

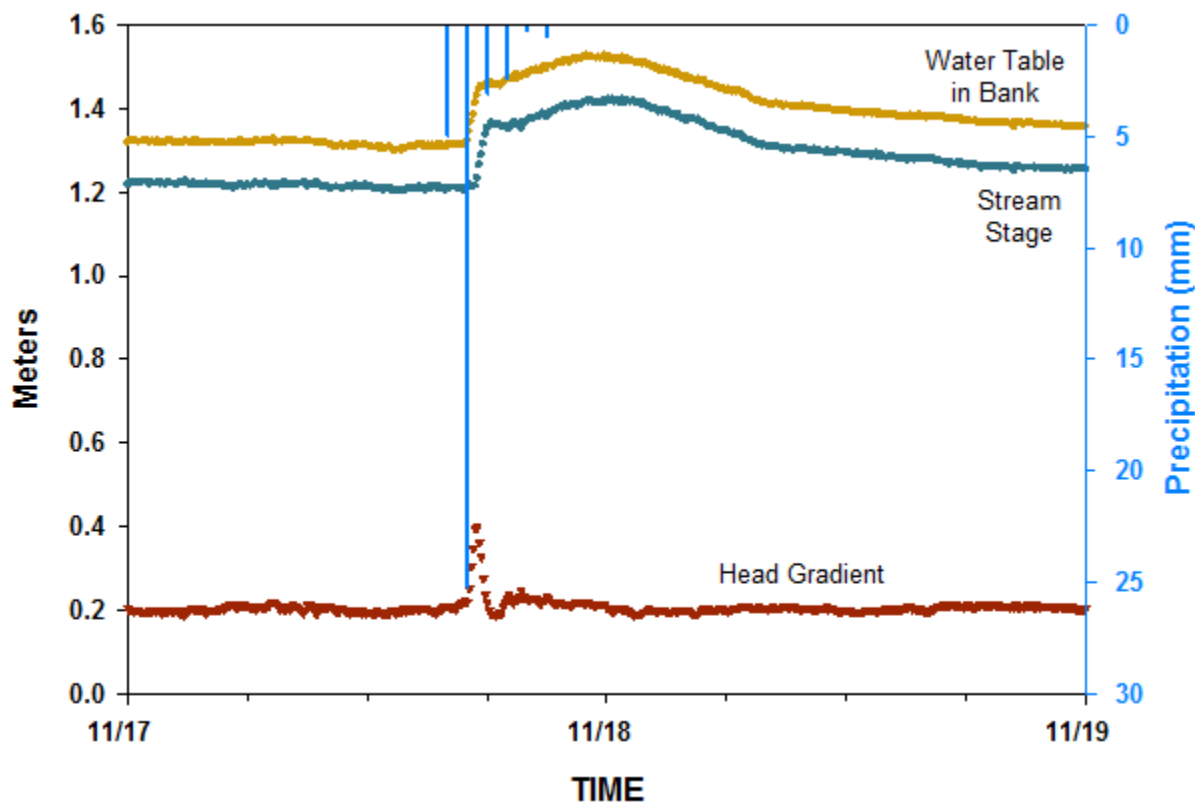


**Figure 3.14.** Stream stage, water table elevation and head gradient during storm starting November 17, 2014

### 3.4 Effects of Storm Intensity and Duration on Nitrate Flux

In order to observe how duration affected  $\Delta J_{NO_3}$ , storm duration and flood duration were plotted against change in nitrate flux (Figure 3.15 and 3.16). Storm duration had no correlation with nitrate flux ( $r = 0.23$ ) because similar storm durations resulted in completely different changes in nitrate flux. While both the November 1<sup>st</sup> and the January 28<sup>th</sup> storms lasted 4 hours, the changes in nitrate flux during the storm were completely different (-0.00238kg and 36.0kg, respectively)(Table 3.1). Flood duration, the time a flood wave takes to pass, had a better relationship with  $\Delta J_{NO_3}$  with an  $r$  value of 0.68. For the most part, as flood duration increased, nitrate flux over base flow conditions increased concomitantly.

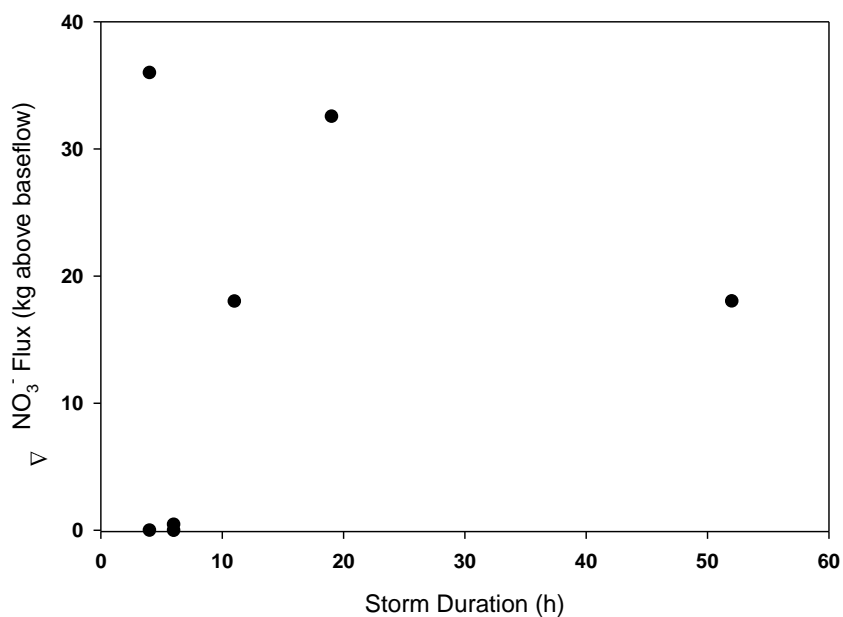


**Figure 3.15.** Storm duration (h) of storms captured between October 22, 2014 and January 20, 2015 plotted against their respective changes in nitrate flux (kg).  $r$  value was 0.23.

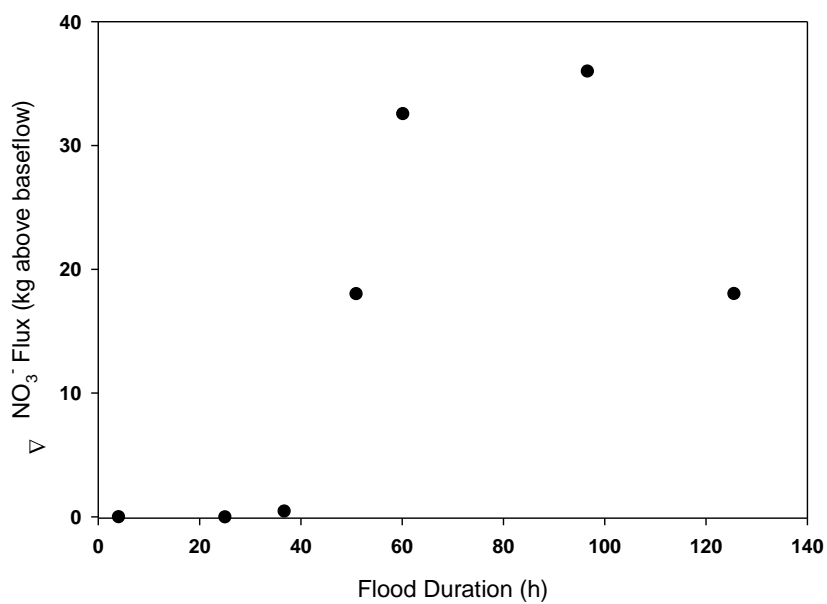


**Figure 3.16.** Duration of flood wave (h) of storms captured between October 22, 2014 and January 20, 2015 plotted against their respective changes in nitrate flux (kg).  $r$  value was 0.68.

Storm intensity was described using the following parameters: total precipitation (mm), peak hourly intensity ( $\text{mm h}^{-1}$ ), flood wave height (cm) and change in discharge ( $\text{m}^3$ ). In order to observe how storm intensity affected nitrate flux, these parameters were plotted against change in nitrate flux (kg). There was no correlation between total precipitation and change in nitrate flux (Figure 3.17). The highest levels of total precipitation, 34.8mm and 36.7mm, resulted radically different changes in nitrate flux, 0.454kg and 32.6kg. Additionally, there was no correlation between hourly peak intensity and change in nitrate flux (Figure 3.18). Similar peak hourly intensities of  $2.5\text{mm h}^{-1}$  yielded radically different  $\Delta J_{\text{NO}_3}$ , viz.,  $-0.0091\text{kg}$  and  $32.6\text{ kg}$ .

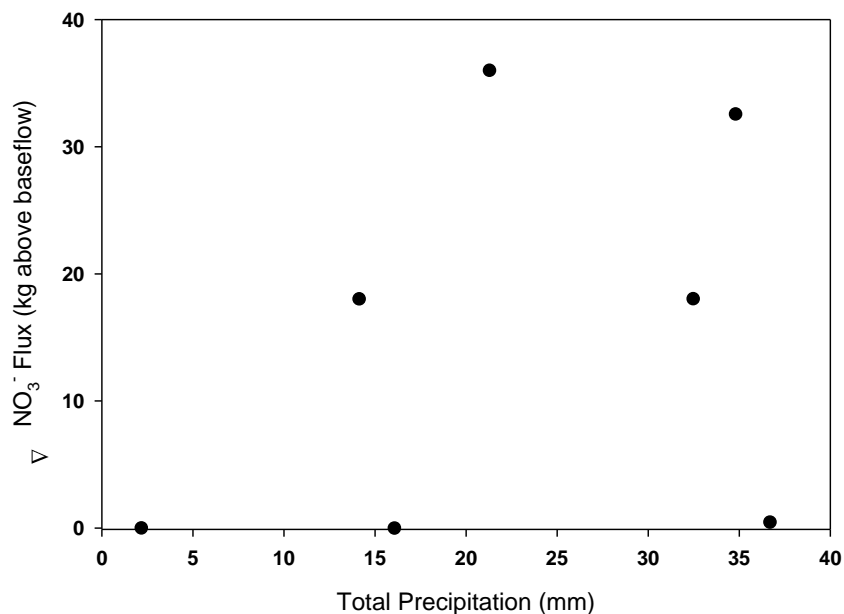


**Figure 3.17.** Total precipitation (mm) of storms captured between October 22, 2014 and January 20, 2015 plotted against their respective changes in nitrate flux (kg). The r value was 0.33.

The change in nitrate flux ( $\Delta J_{\text{NO}_3}$ ) was also plotted against the change in discharge (Figure 3.19). Low changes in discharge ( $22.9\text{ m}^3$  and  $-0.569\text{ m}^3$ ) resulted in the lowest changes in nitrate flux ( $-0.0091\text{kg}$  and  $-0.0024\text{kg}$ ). Then, as  $\Delta Q$  increased,  $\Delta J_{\text{NO}_3}$  increased exponentially

to 20,300m<sup>3</sup> and its maximum change in nitrate flux of 36.0kg was reached. After this maximum, nitrate flux change decreased down to 32.6kg as  $\Delta Q$  increased to 29,900 m<sup>3</sup>.

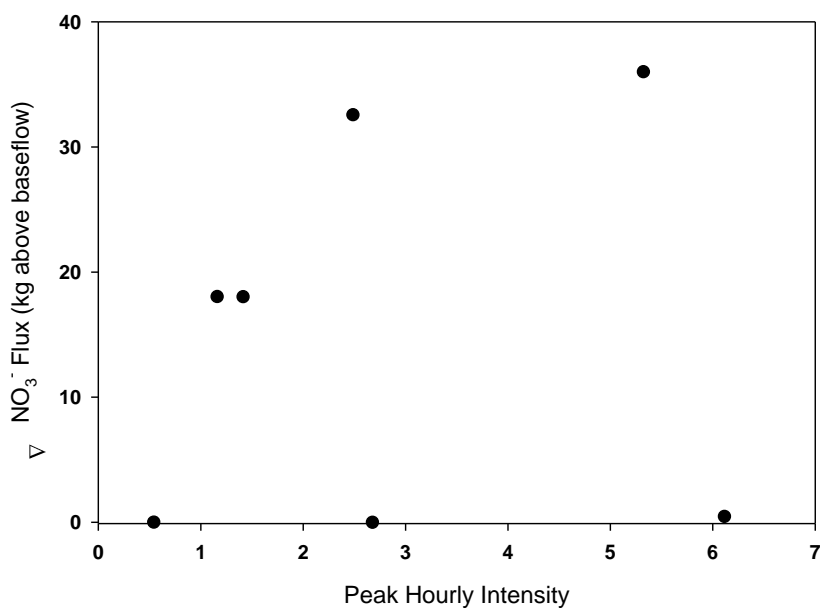


**Figure 3.18.** Peak hourly intensity (mm h<sup>-1</sup>) of storms captured between October 22, 2014 and January 20, 2015 plotted against their respective changes in nitrate flux (kg). r value was 0.13.

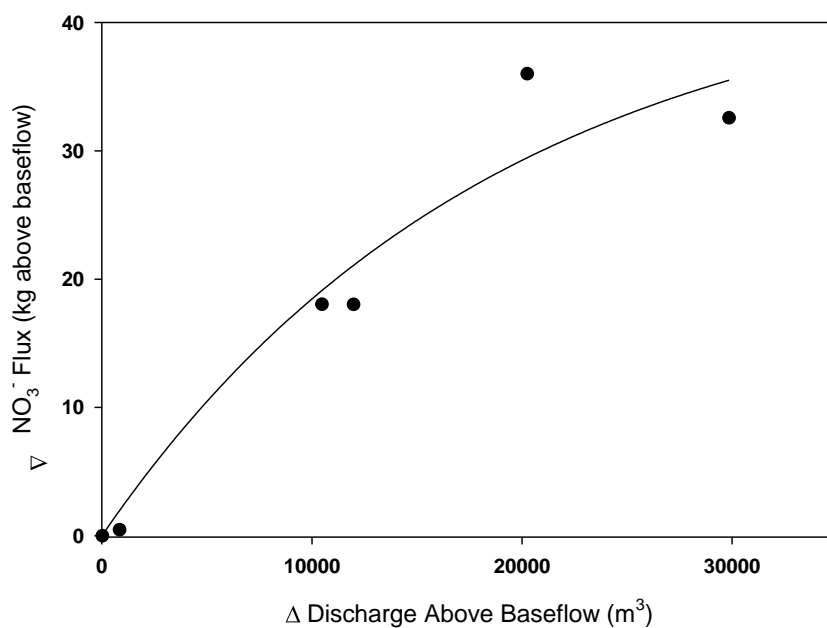


**Figure 3.19.** Change in discharge of storms captured between October 22, 2014 and January 20, 2015 plotted against their respective changes in nitrate flux (kg). Adding an exponential trend line with a maximum rise, the r value was 0.95.

The change in nitrate flux ( $\Delta J_{\text{NO}_3}$ ) was also plotted against the height of flood wave (Figure 3.20). Small flood waves (3.60cm and 7.54cm) resulted in relatively low changes in nitrate flux (-0.00238kg and -0.00909kg) (Table 3.1). At a flood wave of 16.2cm, the change in nitrate flux was at its maximum (36.0kg). After this maximum point, the behaviors of larger flood waves diverged. At flood waves of 21cm, changes in nitrate flux either decreased drastically to 0.454kg or decreased minimally to 32.6kg (Table 3.1).

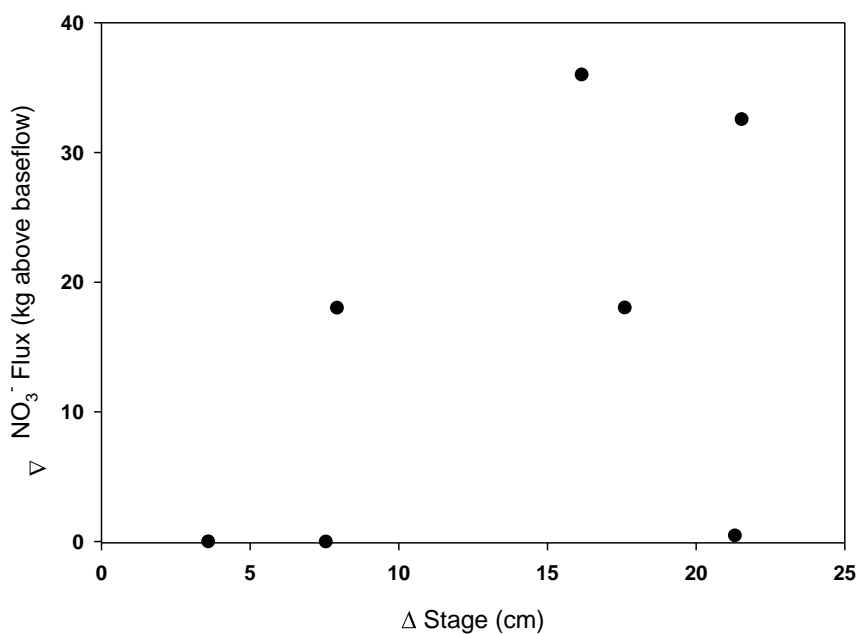


**Figure 3.20.** Flood wave height of storms captured between October 22, 2014 and January 20, 2015 plotted against their respective changes in nitrate flux.  $r$  value was 0.55.

## Chapter 4. Discussion

### 4.1 Influence of Hydraulic Gradients on Discharge and Nitrate Concentration

In Cobb Mill Creek, the hydraulic gradient between the adjacent hillslope and the stream affected rates of discharge and consequently nitrate concentrations as a result of changes in residence time of the nitrate-rich and discharging groundwater in the upper part of the bed sediments where denitrification removes substantial amounts of the nitrate [Gu *et al.*, 2008 and Robertson, 2009]. A decrease in head gradient to the stream will slow discharge, prolonging residence times and nitrate removal. Conversely, an increase in the head gradient will speed up discharge, reducing residence times and nitrate removal. Changes in the nitrate concentration in the water discharging to the stream do not occur instantaneously because it takes time for groundwater discharge to move through stream bed sediments [Robertson, 2009]. During a storm event, both changes in head gradient and changes in nitrate concentration in the stream were observed, but the alteration of the nitrate concentration lagged the flood wave by several hours (Figure 4.1). The change in the head gradient between the stream bank and the stream occurred simultaneously with the change in discharge because they are physical processes directly dependent on the rainfall. At the same time, nitrate concentration decreased rapidly presumably due to the dilution from rainfall and discharge of local water from the stream banks. That local water has a substantially lower nitrate concentration than the water discharging through the sediments, as the source of the water coming from the stream bed is water draining from the upland agricultural fields rather than local water derived from precipitation [Gu, *et al.* 2008]. Subsequently, the high discharge induced from the increase in the hydraulic gradient between the hillslope and the stream flushed out groundwater with a higher concentration of nitrate than during base flow due to the reduced residence time in the zone of active denitrification

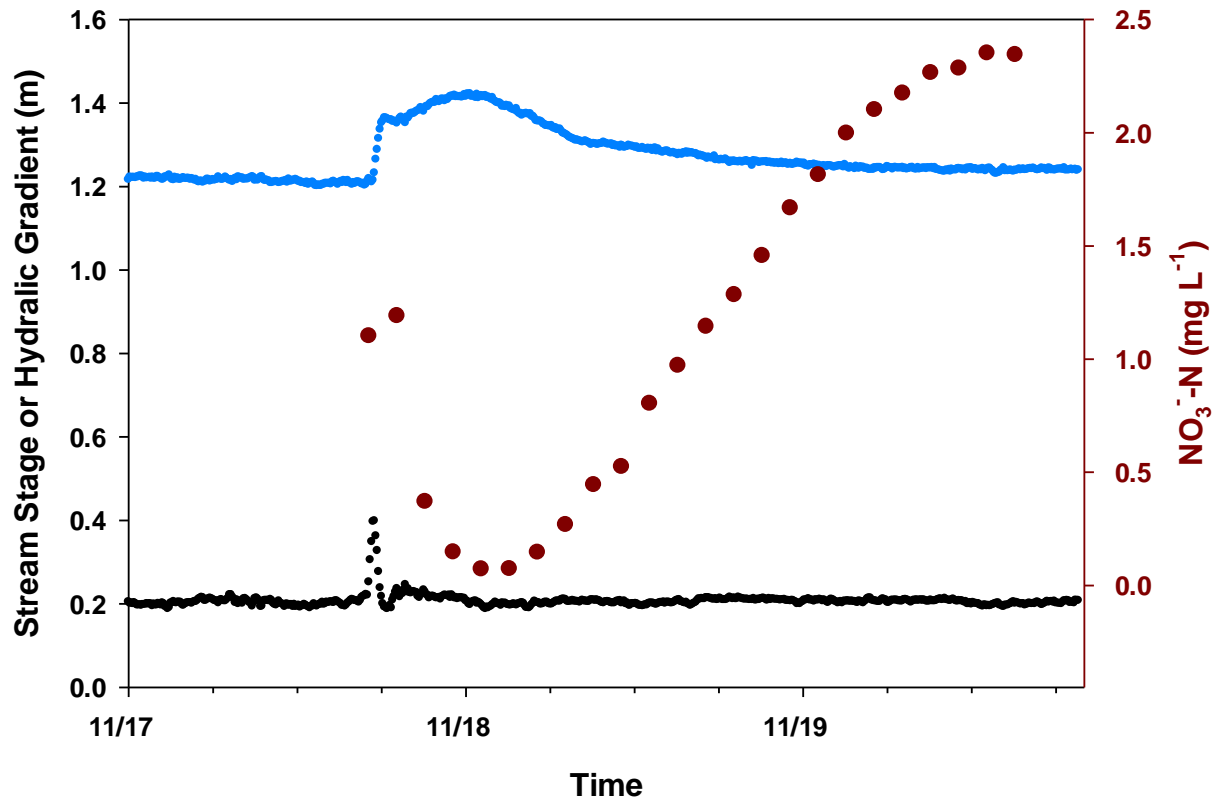


**Figure 4.1** Hydraulic gradient, nitrate concentration in hourly samples, and continuous discharge for the storm event on November 17, 2014.

[Robertson, 2009; Reid-Black, 2014; Gu et al., 2008; Mills et al., 2011; Flewelling et al., 2012].

That process is not instantaneous, however, so the increasing levels of nitrate occurred as stream discharge was returning to base flow. Concentrations continued to increase even when there was little change in the hydraulic gradient due in part to the lack of dilution water, and in part due to the higher nitrate that had built up in the water passing through the streambed more rapidly during the period of greatest difference in the hydraulic gradient, i.e., during the period of maximum discharge represented by the peak in the hydrograph.

The hydraulic gradient can affect rates of discharge and nitrate concentrations but there is a threshold where the hydraulic gradient can no longer be a good predictor of the fates of

discharge and nitrate. The storm needs to have enough precipitation to raise the stage and create a strong enough hydraulic gradient. For example, the storm starting on October 22, 2014 (Figure 3.12) exhibited no large changes in the hydraulic gradient because there was not enough precipitation to raise the flood wave height. Precipitation was directly related to the flood wave height (Figure 4.2). The October 22<sup>nd</sup> storm had 16.1mm of rain which produced a flood wave height of 7.54cm while the November 17<sup>th</sup> storm had 36.7mm of rain that yielded a flood wave of 21.3cm in height. As a result of the lack of change in the hydraulic gradient, the October 22<sup>nd</sup> storm had no major changes in discharge at the flood wave: only a 22.9m<sup>3</sup> increase over the period of the storm (Table 3.1).

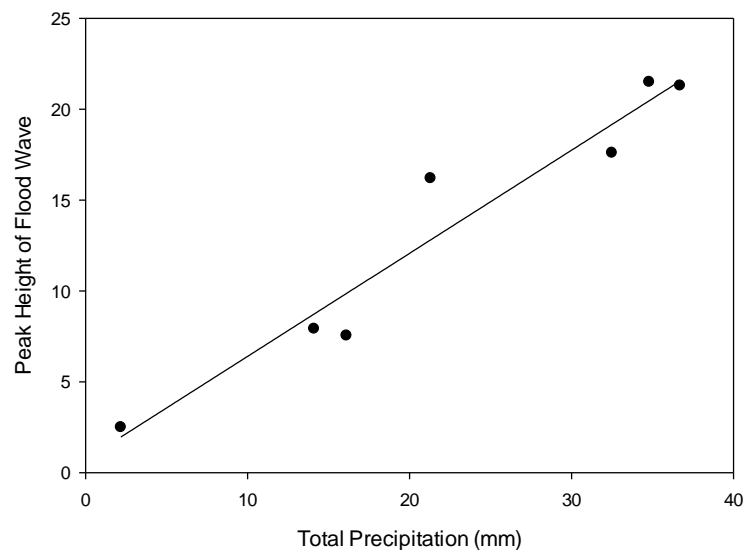


**Figure 4.2.** Linear relationship between total precipitation (mm) and height of flood wave (cm). This relationship has a high  $r^2$  of 0.94.

## 4.2 Effects of Storm Intensity and Duration on Nitrate Flux

According to Gu et al. [2008], a small flood wave should result in a net decrease in the nitrate flux because small flood waves slow discharge through the sediment, yielding longer

residence times and more  $\text{NO}_3^-$  removal. On the other hand, larger flood waves leads to a net increase in  $\text{NO}_3^-$  flux. The elevated stage causes recharge of the groundwater into stream bed and bank sediments. That recharge water is oxygenated which inhibits denitrification. In addition, on the recession limb of the hydrograph, discharge from the groundwater to the stream increases, reducing the residence time of the water in the denitrifying sediments, leading to lower residence times and less  $\text{NO}_3^-$  removal [Gu *et al.*, 2008]. The nine storm events studied in this project followed these patterns to an extent, however flood wave height was not the only determining factor of  $\text{NO}_3^-$  flux. Flood duration which influenced change in discharge,  $\Delta Q$ , also affected change in  $\text{NO}_3^-$  flux ( $\Delta J_{\text{NO}_3}$ ). Figures 3.19 and 3.20 demonstrated that small storms characterized by small flood waves and slowed discharge resulted in a decrease in  $\text{NO}_3^-$  flux while large storms characterized by large flood waves had various discharges which resulted in disparate increases in  $\text{NO}_3^-$  flux.

Small flood waves with a height of 3.60cm - 7.54cm had very small values for  $\Delta Q$  ( $-0.569\text{m}^3$  and  $22.9\text{m}^3$ ). Over the duration of these storms, these  $\Delta Q$  values were probably not different from  $0\text{ m}^3$  meaning that the stream discharges resulting from these events were indistinguishable from base flow. These small flood waves with low storm discharges resulted in relatively low changes in  $\text{NO}_3^-$  fluxes of  $-0.0091\text{kg}$  and  $-0.0024\text{kg}$  (Table 3.1) because slower discharges created longer residence times for the removal of more groundwater nitrate. A negative change in  $\text{NO}_3^-$  flux meant that there was less  $\text{NO}_3^-$  transported by the stream during the storm than at base flow before the storm. This could result from the combination of the dilution of stream water by precipitation as well as by enhanced denitrification. However, since there appeared to be very little water added to the stream, enhanced denitrification is most likely responsible for the negative  $\text{NO}_3^-$  flux.

As the height of the flood wave in several storm events increased toward 16.2cm,  $\Delta Q$  increased to 20,300m<sup>3</sup> and  $\Delta J_{\text{NO}_3^-}$  increased to its maximum of 36.0kg. As shown in the many storms collected (Figure 3.3 - 3.7),  $\text{NO}_3^-$  concentrations decreased at the peak of the storm. Because  $\text{NO}_3^-$  flux is the product of  $\text{NO}_3^-$  concentration and water flux, and because the water flux (total discharge) was high, the high discharge overrode the decrease in  $\text{NO}_3^-$  concentration to yield a greater  $\text{NO}_3^-$  flux during the storm. The high discharge of 20,300m<sup>3</sup> during the storm reduced residence times by quickly flushing out the more concentrated groundwater nitrate. In addition to shorter residence times, nitrate concentrations increased because of inadequate time for denitrification. Higher flood waves allowed oxygenated stream water to recharge stream bed sediments, and oxygen inhibits the conversion of  $\text{NO}_3^-$  to  $\text{N}_2$  gas through denitrification.

At the highest flood waves of 21cm, while  $\Delta J_{\text{NO}_3^-}$  ultimately decreased from its maximum of 36.0kg (Table 3.1), change in discharge and nitrate flux behaviors began to diverge because flood wave size alone was not the only factor determining  $\text{NO}_3^-$  flux. Nitrate flux decreased possibly because of dilution. Dilution of  $\text{NO}_3^-$  by precipitation was occurring during all the storms but perhaps dilution had a larger effect during these increased flood wave heights because the largest amounts of precipitation created these large 21cm flood waves. Figure 4.2 shows that as total precipitation increased, the flood wave height increased linearly. The largest flood waves (21.3cm and 21.5cm) had the largest total precipitation records (36.7mm and 34.8mm) (Table 3.1). Discharge above base flow during those two events either increased to 842m<sup>3</sup> or increased to 29,900m<sup>3</sup>. These disparate changes in discharge were a result of changes flood duration which changed peak hourly rainfall intensities. Discharge during the November 17<sup>th</sup> storm decreased back down to 842m<sup>3</sup> because of a combination of high stream stage and short flood duration. A short flood duration created high rainfall intensity of 6.11mm h<sup>-1</sup>. This high intensity was able to

cause a sharp rise in the stream stage thereby lowering the gradient between the high stream stage and the water table elevation in the stream bank. The result, then, was a reduced  $\Delta Q$  to 842  $\text{m}^3$  thus allowing more time for nitrate removal and reducing  $\Delta J_{\text{NO}_3}$  back down to 0.454kg (Table 3.1).

On the other hand, during the December 24<sup>th</sup> storm, a similar sized flood wave (21.5cm) resulted in a much bigger change in discharge (29,900 $\text{m}^3$ ) and a bigger change in nitrate flux (32.6kg). Perhaps, head gradients did not play as significant a role because flood duration was half as long as the duration for the November 17<sup>th</sup> storm. As a result, peak hourly intensity was 4 $\text{mm h}^{-1}$  lower than the intensity during the November 17<sup>th</sup> storm (Table 3.1). Slower rainfall might infiltrate better, preventing the stream stage to rise higher than the water table. As exemplified in Figure 3.14, during high flood waves, the water table elevation can increase faster than the stream stage. Within an hour, the stream stage changed from 1.21m to 1.23m while the water table jumped from 1.31m to 1.43m (Figure 3.14). Water table elevation increased at a faster rate because vertical infiltration into the stream bank was faster than the rise in the stream stage. The sandy soils of stream bank with its high porosity [Gu *et al.*, 2008] allowed for fast infiltration. On the other hand, the meandering stream had no rigid stream channel and could overflow and expand horizontally and not necessarily vertically, resulting in a lower stream stage. This slow rise in stage but fast rise in water table increased head gradients and allowed for fast discharge (29,900 $\text{m}^3$  over base flow) and thus more rapid flushing of nitrate (32.6kg).

#### *Other storm parameters*

Based on the nine storms sampled, there was no correlation between peak hourly intensity, total precipitation and nitrate flux (Figure 3.17 and 3.18) however peak intensity and

total precipitation did affect nitrate flux indirectly. As explained previously in the disparate nitrate fluxes for similar flood waves, peak intensity played a pivotal part in hydraulic gradients. High peak intensity allowed stream stage to rise higher in relation to the usually quickly rising water table elevation, reducing the head gradient and lowering discharge and nitrate concentration. Low precipitation intensity resulted in a slow rise of the stream stage in relation to the quickly rising water table elevation, creating larger head gradient and increasing discharge and nitrate concentration. Total precipitation did not directly affect nitrate flux however it did affect the flood wave height. As total precipitation increased, the flood wave height increased linearly (Figure 4.2). As more rain fell, the stream stage was able to rise higher and increase discharge to a certain extent.

Storm duration had no correlation ( $r$  value was 0.23) with nitrate flux while flood duration had a correlation ( $r$  value was 0.68) with nitrate flux. Storm duration did not indicate how the nitrate flux behaved because same storm durations resulted in completely different changes in nitrate flux (Figure 3.15). Flood duration was a better indicator because flood duration took into account the actual condition of the stream stage and determined change in discharge,  $\Delta Q$ . The excellent correspondence between change in discharge and change in nitrate flux,  $\Delta J_{NO_3}$  (Figure 3.19), suggests that  $\Delta J_{NO_3}$  was not solely dependent on the height of the flood wave but also flood duration. The height of a flood wave only controls instantaneous discharge; however total discharge (water flux) was combination of the flood wave height and flood duration.

### **4. 3 Patterns in non-storm events**

Even during non-storm events, the same mechanisms between hydraulic gradient, discharge and nitrate were present. In July, vegetation was abundant and evapotranspiration was

functioning actively according to the availability of sunlight from day to night. In the day time, due to the evapotranspirative demand of water, the nearby water table was being drawn down [Robertson, 2009; Reid-Black, 2014]. This lowering of the water table resulted in the reduction of gradient between the stream and water table, reducing the rate of groundwater discharge through the sediments to the stream. Much like the mechanics described during a storm, the slower discharges increased the residence time in the zone of denitrification and thus increased nitrate removal. Nitrate concentrations showed a lag [Robertson, 2009], not dissimilar to what was observed in this study (Figure 3.10), when nitrate decreased later on in the night even though slower discharges were occurring during the day time. Diurnal drawdowns of the water table created diurnal variations in nitrate removal [Robertson, 2009]. At the end of September, there was less evapotranspiration because the leaves were senescing and starting to fall. As a result, there were no marked diurnal drawdowns of the water table and thus no diurnal fluctuation in nitrate (Figure 3.11).

#### **4.4 Project Relationship to Larger Scope**

The transport of dissolved nitrogen compounds from coastal groundwater to streams draining to the coastal lagoons creates problems of eutrophication in the shallow marine and estuarine environments [Denver *et al.*, 2003 as cited by Gu *et al.*, 2007]. In agricultural environments, most of the sources of nitrogen come from nitrate fertilizer applications [Smil, 1997; Evans, 1996 as cited in Robertson, 2009]. In order to resolve these issues of eutrophication, the amount of  $\text{NO}_3^-$  that flows from the uplands and agricultural fields into the coastal lagoon must be known. Concentration measurements solely from the uplands do not provide an accurate estimation of  $\text{NO}_3^-$  because of the biogeochemical reactions that occur near the groundwater - surface water interface (GSI) [Reid-Black, 2014; Flewelling *et al.*, 2012; Robertson, 2009; Gu *et*

*al.*, 2007; *Gu et al.*, 2008; *Hedin et al.*, 1998]. As groundwater originating from the uplands moves through the GSI to the stream, denitrification can alter original  $\text{NO}_3^-$  concentrations. However, measurements solely from the stream at base flow also do not provide an accurate estimate of  $\text{NO}_3^-$  concentrations flowing to the coastal lagoons. As depicted in the results of this project, the passage of a flood wave changes the  $\text{NO}_3^-$  flux. Depending on the flood wave size and duration, change in  $\text{NO}_3^-$  flux compared at base flow can either increase or decrease. Thus, in order to accurately predict how much  $\text{NO}_3^-$  drains to the coastal lagoons, future  $\text{NO}_3^-$  watershed budgets need to take into account storm events and more importantly the magnitude of the storm. With a more complete understanding of nitrate transport, better nitrogenous fertilizer applications can be recommended to ultimately better protect our coastal environment.

#### **4.5 Future Research**

In order to predict accurately nitrate fluxes in shallow marine and estuarine environments, more storms of various magnitudes need to be collected. Only 7 storms (October 22<sup>nd</sup> - January 18<sup>th</sup>) were used to examine the relationship between storm intensity, duration and change in nitrate flux. Sampling more storms would provide more data points to help strengthen the argument that flood wave height and duration affect change in nitrate flux. Capturing a major storm, such as a hurricane, would also provide an extreme example of a large flood wave height and long duration much needed to analyze a spectrum of storm magnitudes. More sampling of smaller storms would also provide further insight to negative changes in nitrate flux. With more data points, modeling results can be verified. A current model for Cobb Mill Creek made by *Gu et al.*, [2008] only takes into account flood wave height when determining nitrate flux during a storm. In the absence of data, that model predicted that stage increases of 10 cm would result in lowered flux of  $\text{NO}_3^-$  in the stream when compared to an equal amount of time at base flow.

This study demonstrates that the situation is more complex than one in which increased stage is the only controlling variable as in Gu's model. The high correlation of  $\Delta J_{\text{NO}_3}$  with  $\Delta Q$ , the change in discharge, points to at least one more variable that must be taken into account when predicting changes in  $\text{NO}_3^-$  flux, and that is flood duration. Therefore, in order to predict future nitrate flux during a storm more accurately, Gu's [2008] model should be tested after modification to include flood duration against an expanded data set beginning with those data gathered here. If the modified model can more accurately predict  $\Delta J_{\text{NO}_3}$ , then model could be used to alter annual flux calculations for hydrographs generated in streams of the Eastern Shore, and perhaps a large set of coastal streams in general.

## References

- Bachman L.J., B. Lindsey, J. Brakebill, and D.S. Powars (1998), Ground-water discharge and base-flow nitrate loads of nontidal streams, and their relation to a hydrogeomorphic classification of the Chesapeake Bay watershed, Middle Atlantic Coast, *US Geological Survey*, 03–4059.
- Chen, R.L., Keeney, D.A., Graetz, D.A., and A.J. Holding (1972), Denitrification and nitrate reduction in Wisconsin lake sediments, *Journal of Environmental Quality*, 1, 5.
- Cowling, E. B. and J. N. Galloway (2002). Reactive nitrogen and the world: 200 years of change, *Ambio*, 31: 641io.
- Creed, I. F., Band, L. E., Foster, N.W., Morrison, I.K., Nicolson, J.A., Semkin, R.S., Jeffries, D.S., 1996. Regulation of nitrate-N released from temperate forests: A test of the N-flushing hypothesis. *Water Resour. Res.* 32, 3337-3354.
- Croen, L.A., K. Todoroff, and G.M. Shaw (2001), Maternal exposure to nitrate from drinking water and diet and risk for neural tube defects, *American Journal of Epidemiology*, 153, 7.
- Denver, J.M., S.W. Ator, L.M. Debrewer, M.J. Ferrari, J.R. Barbaro, T.C. Hancock, M.J. Brayton, M.R. Nardi (2003), Water quality in the delmarva peninsula: Delaware, Maryland, and Virginia, *US Geological Survey*, 1228, 1999–2001.
- EPA, U.S., and USDA (1998), Clean Water Action Plan: restoring and protecting America's waters, Clean Water Action Plan: Washington D.C., US EPA/USDA.
- Evans, L.T. (1996), *Crop Evolution, Adaptation, and Yield*: Cambridge: Cambridge University Press, 512.
- Flewelling, S. A. (2009), Nitrogen storage and removal in catchments on the eastern shore of Virginia, PH.D. Dissertation, University of Virginia.
- Flewelling, S. A., G. M. Hornberger, J. S. Herman, and A. L. Mills (2012), Travel time controls the magnitude of nitrate discharge in groundwater bypassing the riparian zone to a stream on virginia's coastal plain, *Hydrol. Process.*, 26, 1242-1253, DOI: 10.1002/hyp.8219.
- Freeze, R., and J. Cherry (1979), *Groundwater*. Englewood Cliffs: Prentice Hall, 604.
- Gribovski, Z., Kalicz, P., Szilagyi, J., and Kucsara, M. (2008), Riparian zone evapotranspiration estimation from diurnal groundwater level fluctuation, *Journal of Hydrology*, 349, 6-17.
- Gu, C., G. M. Hornberger, A. L. Mills, J. S Herman, and S. A. Flewelling (2007). Nitrate reduction in streambed sediments: Effects of flow and biogeochemical kinetics. *Water Resour. Res.*, 43, W12413, doi:10.1029/2007WR006027.
- Gu, C.; G.M. Hornberger, A.L. Mills, and J.S. Herman, (2008), Influence of stream-aquifer interactions in the riparian zone on nitrate flux to a low-relief coastal stream. *Water Resour Res.*, 44.
- Gu, C., G. M. Hornberger, J. S. Herman, and A. L. Mills (2008), Effect of freshets on the flux of groundwater nitrate through streambed sediments, *Water Resour. Res.*, 44, W05415, doi:10.1029/2007WR006488.
- Hedin, L., J. von Fischer, N. Ostrom, B. Kennedy, M. Brown, and G. Robertson (1998), Thermodynamic constraints on nitrogen transformations and other biogeochemical processes at soilstream interfaces, *Ecology*, 79, 684-703.
- Hill, M.K. (1997), *Understanding Environmental Pollution*: Cambridge: Cambridge University Press, 334.

- Hill, A., K. Devito, S. Campagnolo, and K. Sanmugadas (2000), Subsurface denitrification in a forest riparian zone: interactions between hydrology and supplies of nitrate and organic carbon, *Biogeochemistry*, 51, 193-223.
- Lowrance, R., R. Todd, J.J. Fail, O.J. Hendrickson, R. Leonard, and L. Asmussen (1984), Riparian forests as nutrient filters in agricultural watersheds, *Bioscience*, 34, 4.
- Lowrance, R (1992), Groundwater nitrate and denitrification in a coastal plain riparian forest, *Journal of Environmental Quality*, 21, 401-405.
- Mills, A.L., J.S. Herman, and A. Anutaliya, (2011), Sediments as filters of applied nitrogen from discharging groundwater to low-relief coastal streams. *Coastal and Estuarine Research Federation*. Daytona Beach, FL.
- McGlathery, K. J., K. Sundback, and I. C. Anderson (2007), Eutrophication in shallow coastal bays and lagoons: the role of plants in the coastal filter, *Mar. Ecol. Prog. Ser.*, 348, 1-18, 10.3354/meps07132.
- Pickus, B. A., Herman, J. S., and Mills, A. L (2014). Building rating curves for low-order streams draining small watersheds of the Atlantic Coastal Plain. Geological Society of America, Southeastern Section Meeting, April 10-11, 2014, Blacksburg, VA. *Geological Society of America, Abstracts with Programs*, 46, 18.
- Reid-Black, K. (2014), Periodic changes in the nitrate concentration of stream water in a low-relief coastal stream, MS Thesis, University of Virginia, 141.
- Roberston, W.M (2009), Diurnal variations in nitrate concentrations in the Cobb Mill Creek, VA. MS Thesis, University of Virginia.
- Sawyer, A.H., L.A. Kaplan, O. Lazareva, and Michael, H.A. (2014) Hydrologic dynamics and geochemical responses within a floodplain aquifer and hyporheic zone during Hurricane Sandy. *Water Resour Res.* 50, 4877-4892, doi: 10.1002/2013WR015101
- Simmons, R. C., A. J. Gold, and P. M. Groffman (1992). Nitrate Dynamics in Riparian Forests - Groundwater Studies, *Journal of Environmental Quality*, 21: 659-665.
- Smil, V (1997), Global population and the nitrogen cycle, *Scientific American*, 277, 6.
- Speiran, G.K. (1996), Geohydrology and geochemistry near coastal groundwater-discharge areas of the Eastern Shore, Virginia, *US Geological Survey*, 2479.
- Vidon, P.G.F., and A.R. Hill (2004), Landscape controls on the hydrology of stream riparian zones, *Journal of Hydrology*, 292, 210-228.
- Weibe, K., and N. Gollehon (2006), Agricultural resources and environmental indicators, USDA. *Agricultural Resources and Environmental Indicators, 2006 Edition*, EIB-16, U.S. Department of Agriculture, Economic Research Service.
- Williams, M., A. Buda, H. Elliott, J. Hamlett, E. Boyer, J. Schmidt (2014). Groundwater flow path dynamics and nitrogen transport potential in the riparian zone of an agricultural headwater catchment, *Journal of Hydrology*, 511: 870-879.
- Willems, H.P.L., M.D. Rotelli, D.F. Berry, E.P. Smith, R.B. Reneau, and S. Mostaghimi (1997), Nitrate removal in riparian wetland soils: Effects of flow rate, temperature, nitrate concentration and soil depth, *Water Research*, 31, 841-849.
- Wondzell, S. M., and F. J. Swanson (1996a), Seasonal and storm dynamics of the hyporheic zone of a 4th-order mountain stream. 1: Hydrologic processes, *J. North Am. Benthol. Soc.*, 15, 3-19.
- Wondzell, S. M., and F. J. Swanson (1996b), Seasonal and storm dynamics of the hyporheic zone of a 4th-order mountain stream. 2. Nitrogen cycling, *J. North Am. Benthol. Soc.*, 15, 20-34.

- Zhang, Y., F. Li, Q. Zhang, J. Li, Q. Liu (2014). Tracing nitrate pollution sources and transformation in surface- and ground-waters using environmental isotopes, *Science of The Total Environment*, 490: 213-224.
- Zumft, W (1997), Cell biology and molecular basis of denitrification, *Microbiology and Molecular Biology Reviews*, 61, 533-616.